DEVELOPMENT OF A MULTIPLE BEAM COMBINER USING STIMULATED RAMAN SCATTERING IN MULTIMODE FIBER

THESIS

Brian M. Flusche, 1st Lieutenant, USAF

AFIT/GAP/ENP/06-04

DEPARTMENT OF THE AIR FORCE
AIR UNIVERSITY

AIR FORCE INSTITUTE OF TECHNOLOGY

Wright-Patterson Air Force Base, Ohio

AFIT/GAP/ENP/06-04

DEVELOPMENT OF A MULTIPLE BEAM COMBINER USING STIMULATED RAMAN SCATTERING IN MULTIMODE FIBER

THESIS

Presented to the Faculty

Department of Engineering Physics

Graduate School of Engineering and Management

Air Force Institute of Technology

Air University

Air Education and Training Command

In Partial Fulfillment of the Requirements for the

Degree of Master of Science (Applied Physics)

Brian M. Flusche, BS

1st Lieutenant, USAF

March 2006

AFIT/GAP/ENP/06-04

DEVELOPMENT OF A MULTIPLE BEAM COMBINER USING STIMULATED RAMAN SCATTERING IN MULTIMODE FIBER

Brian M. Flusche, BS

1st Lieutenant, USAF

Approved:

Thomas G. Alley (Chairman)	21 Feb 06 date
Matthew J. Bohn (Member)	21 Feb 06 date
Timothy H. Russell (Member)	21 FEB 2006 date

Abstract

Beam combination was demonstrated by splitting the beam from a diode pumped Q-switched Nd:YAG laser and pumping a multiple input, single output fiber squid. Beam cleanup of the resulting output beam using stimulated Raman scattering was then demonstrated in both 100 μm fiber (Stokes $M^2 = 1.86$) and 200 μm fiber (Stokes $M^2 = 1.40$). The performance of the 200 μm fiber was compared to that of the 100 μm fiber.

Energy conversion efficiency into the Stokes beam was measured as a function of input energy and found to be limited by the attenuation characteristics of the fiber. When input energy was increased, the conversion efficiency of pump energy to Stokes energy decreased. In the 100 μm fiber, the pump-to-Stokes conversion efficiency decreased from a high of 44% to a low of 16% as input pump energy increased. In the 200 μm fiber, the pump-to-Stokes conversion efficiency decreased from a high of 19% to a low of 12% as input pump energy increased. For a given input pump energy, the 200 μm fiber was more efficient than the 100 μm fiber.

Beam quality was measured via the M^2 fit parameter as a function of input energy and was found to slightly degrade in both fibers as input energy increased. In addition, beam quality was measured as a function of 100 μm fiber length and determined to degrade slightly ($M^2 < 2.5$) at fiber lengths less than 400 m. Additional fiber length beyond 400 m did not improve beam quality and reduced output energy, although the Stokes threshold was reduced.

Acknowledgments

I would like to express my sincere appreciation to my faculty advisor, Lt Col Thomas Alley, for his guidance and support throughout the course of this thesis effort. The clear objectives, insight, and experience were certainly appreciated. I would also like to thank Dr. Won Roh and Maj Timothy Russell for their patient advice. The in-depth explanations helped me to much better understand the theoretical aspects of this work. I would like to thank Capt Brent Grime and Capt Nathan Terry for their assistance and advice with regard to lab techniques. The tips and tricks saved me a great deal of time in setting up the experiments. I would also, like to thank my sponsors: the High Power Solid State Lasers Branch, Laser Division, Directed Energy Directorate, Air Force Research Lab (AFRL/DELO), Dr. Schlossberg at the Air Force Office of Scientific Research, Physics and Electronics (AFOSR/NE), and the AFIT Faculty Research Council as well as the Engineering Physics department, for both the support and latitude provided to me in this endeavor.

Brian M. Flusche

Table of Contents

Page

Abstract iv

Acknowledgments v

Table of Contents vi

List of Figures viii

1 Introduction 1

1.1 Chapter Overview 1
1.2 Background 1
1.3 SRS Theory 2
1.4 Research Objectives 4
1.5 Investigative Questions 4
1.6 Limitations 7

2 Literature Review 10

2.1 Chapter Overview 10
2.2 Beam Cleanup 10
2.3 Beam Combining 12
2.4 Summary 12

3 Observation of Beam Cleanup in 100 μm Fiber 14

3.1 Experimental Setup 14
3.2 Results 15
3.3 Summary 16

4 Two Input Channel Fiber Squid Beam Combining and Cleanup 17

4.1 Experimental Setup 17
4.2 Results 19
4.3 Summary 26

5 Four Input Channel Beam Combining and Cleanup with 100 μm Fiber 28

5.1 Experimental Setup 28
5.2 Results 29
5.3 Summary 38

6 Four Input Channel Beam Combining and Cleanup with 200 μm Fiber 40

6.1 Experimental Setup 40

6.2 Results 41
6.3 Summary 49

7 Stokes Beam Quality as Fiber Length Changed 51

7.1 Experimental Setup 51
7.2 Results 52
7.3 Summary 54

8 Graded Index Fiber Compared to Step Index Fiber 55

8.1 Motivation 55
8.2 Experimental Setup 55
8.3 Results 58
8.4 Summary 60

9 Conclusions and Recommendations 62

9.1 Conclusions of Research 62
9.2 Recommendations for Future Research 64

Bibliography 66

List of Figures

Figure Page

1. Energy diagram of Raman Scattering. Incoming photon at frequency ω_p is scattered by a molecule of the medium to a lower frequency Stokes photon ω_s, while the molecule makes a transition to a higher vibrational state, represented by the optical phonon at frequency ω_v. 3

2. Experimental setup for observing beam cleanup in 100 um core fiber. The 1064 nm laser light from the Nd:YAG laser served as the pump for the SRS process in the fiber. The edge filter reflected any residual pump light into a beam dump, ensuring no pump light was present when diagnostics where performed. The wedge served as a pickoff, allowing diagnostics but preventing damage to sensitive equipment. The use of 10x microscope objectives on either end of the fiber resulted in maximum coupling efficiency. 14

3. Spectrum demonstrating peak energy of Stokes beam occurred at 1116.5 nm. 15

4. Spectrum of output as seen after edge filter, showing three orders of Stokes beams and confirming no pump energy is passing through the filter. 16

5. Experimental setup for demonstration of two channel beam combination and cleanup. The 1064 nm laser light from the Nd:YAG laser served as the pump for the SRS process in the fiber. The edge filter reflected any residual pump light into a beam dump, ensuring no pump light was present when diagnostics where performed. The wedge served as a pickoff, allowing diagnostics but preventing damage to sensitive equipment. The use of 16x microscope objectives on either end of the fiber resulted in maximum coupling efficiency. 18

6. Percent conversion efficiency of coupled pump energy into generated Stokes energy. Pump energy of 58 μJ represents channel 1 only. Pump energy of 40 μJ represents channel 2 only. Pump energy of 95 μJ represents both channels in use simultaneously..... 20

7. Measured energy after SRS fiber for different pump configurations. Measured Stokes energy after SRS fiber is represented by diamonds. Measured pump energy reflected off edge filter after SRS fiber is represented by squares. Pump energy of 180 μJ represents channel 1 only. Pump energy of 128 μJ represents channel 2 only. Pump energy of 300 μJ represents both channels in use at the same time. 21

8. Attenuation data for 0.29 NA Flightguide graded index 100 μm multimode fiber used in beam combining and cleanup experiments. Data provided by ThorLabs and included when fiber was delivered. 22

9. M^2 of the generated Stokes beam (vertical stripes) and the transmitted pump beam (diagonal stripes) depending on which channel was used. 23

10. Far field images of generated Stokes and transmitted pump beams. The far field images of the Stokes beams are on the left, while the far field transmitted pump beams are on the right. (Top) Photographs when both channels are in operation simultaneously. (Middle) Channel 1 only. (Bottom) Channel 2 only. All pictures are at 4x zoom. 24

11. Near field images of generated Stokes and transmitted pump beams. The near field images of the Stokes beams are on the left, while the near field transmitted pump beams are on the right. (Top) Photographs when both channels are in operation simultaneously. (Middle) Channel 1 only. (Bottom) Channel 2 only. All pictures are with no zoom applied. 25

12. Experimental setup for demonstration of four channel beam combination and cleanup in 100 μm fiber. The 1064 nm laser light from the Nd:YAG laser served as the pump for the SRS process in the fiber. The edge filter reflected any residual pump light into a beam dump, ensuring no pump light was present when diagnostics where performed. The wedge served as a pickoff, allowing diagnostics but preventing damage to sensitive equipment. The use of 16x microscope objectives on either end of the fiber resulted in maximum coupling efficiency. 28

13. M^2 value of generated Stokes beam (vertical stripes) compared to transmitted pump beam (diagonal stripes) pumping input channels individually and simultaneously. 30

14. M^2 (vertical stripe) compared to generated Stokes energy in μJ (diagonal stripe) pumping input channels individually and simultaneously..... 31

15. Measured Stokes beam M^2 (vertical stripes), calculated weighted average Stokes beam M^2 (horizontal stripes), and measured transmitted pump M^2 value (diagonal stripes) as a function of input channels used. 32

16. Impact of each input channel on M^2 value of generated Stokes beam, as determined by varying which of the four input channels were used and which was blocked. 33

17. Intensity profile of generated Stokes beam, while blocking (a) channel 1, (b) channel two, (c) channel 3, and (d) channel 4. When channel 3 was blocked, (bottom left), the beam looks most like the fundamental mode and distortion of the central intensity region beam was somewhat reduced, becoming more circular. 34

18. M^2 of generated Stokes beam (diamonds) and coupled pump beam (squares) as a function of increasing pump energy coupled into the SRS fiber. 35

19. Percent of coupled pump energy converted into Stokes energy as a function of increasing pump energy. 36

20. Spectrum analyzer sweeps from 1050 nm to 1500 nm demonstrating higher fiber attenuation of higher Stokes orders. For all graphs, wavelength is displayed on the horizontal axis, while the vertical axis is a relative intensity measurement. Graphs are for increasing pump energy coupled into the fiber: (a) At 25 μJ per pulse, the Stokes threshold has been reached. The pump beam is shown at 1064 nm and the 1^{st} order Stokes beam is present at 1116.5 nm. (b) At 35 μJ per pulse, the effects of four-wave mixing become apparent, with three well defined Stokes orders, and hints of a fourth and fifth order. (c) At 90 μJ per pulse, the higher attenuation of the fiber at longer wavelength is shown, as the fifth and sixth Stokes orders are generated, but remain very low in intensity. (d) At 150 μJ per pulse, the relative intensities of the higher Stokes orders are almost unchanged from the sweep shown in (c), confirming the extra energy has been lost in the fiber. 37

21. Generated Stokes energy in the 100 μm fiber as a function of increasing Nd:YAG laser diode pump current. 38

22. Experimental setup for demonstration of four channel beam combination and cleanup. The 1064 nm laser light from the Nd:YAG laser served as the pump for the SRS process in the fiber. The edge filter reflected any residual pump light into a beam dump, ensuring no pump light was present when diagnostics where performed. The wedge served as a pickoff, allowing diagnostics but preventing damage to sensitive equipment. The use of 16x microscope objectives on either end of the fiber resulted in maximum coupling efficiency. 40

23. M^2 of generated Stokes beam (squares) and coupled pump beam (diamonds) as a function of increasing pump energy coupled into the 200 μm SRS fiber..... 42

24. Effect of input pump energy on beam quality of Stokes beam generated in 200 μm fiber as shown by far field pictures of the beam. (a) 110 μJ, M^2 = 9.51 right at the Stokes threshold (b) 139 μJ, M^2 = 1.40 slightly above Stokes threshold (c) 193 μJ, M^2 = 2.02 (d) 303 μJ, M2 = 2.75..... 43

25. Percent of coupled pump energy converted into Stokes energy as a function of increasing pump energy in the 200 μm SRS fiber. 44

26. Spectrum analyzer sweeps from 1050 nm to 1500 nm demonstrating higher fiber attenuation of higher Stokes orders. For all graphs, wavelength is displayed on the horizontal axis, while the vertical axis is a relative intensity measurement. Graphs are for increasing pump energy coupled into the fiber: (a) At 110 μJ per pulse, the Stokes threshold has been reached. The pump beam is shown at 1064 nm and the 1^{st} order Stokes beam is present at 1116.5 nm. (b) At 140 μJ per pulse, the effects of four-wave mixing become apparent, with four well defined Stokes orders. (c) At 170 μJ per pulse, the higher attenuation of the fiber at longer wavelength is shown, as the fifth Stokes order is generated, but remains very low in intensity. (d) At 300 μJ per pulse, the relative intensities of the higher Stokes orders are very similar to the sweep shown in (c), confirming the extra energy has been lost in the fiber. 45

27. Total energy output from 200 μm fiber as a function of increasing pump energy coupled into the fiber. 46

28. M^2 of generated Stokes beam from 100 μm fiber (diamonds) and 200 μm fiber (squares) as a function of increasing pump energy coupled into the fiber. 47

29. Stokes percent conversion as a function of increasing coupled pump energy for 100 μm fiber (diamonds) and 200 μm fiber (squares)..... 48

30. Generated Stokes energy in 100 μm fiber (diamonds) and 200 μm fiber (squares) as a function of pump energy coupled into the fiber. 49

31. Experimental setup for observing beam cleanup in 100 um core size fiber. The fiber spool was cut to a series of different lengths, and the Stokes beam quality was then measured. The 1064 nm laser light from the Nd:YAG laser served as the pump for the SRS process in the fiber. The edge filter reflected any residual pump light into a beam dump, ensuring no pump light was present when diagnostics where performed. The wedge served as a pickoff, allowing diagnostics but preventing damage to sensitive equipment. The neutral density filter (NDF) attenuated the beam to prevent saturation of the camera. The use of 10x microscope objectives on either end of the fiber resulted in maximum coupling efficiency. 51

32. M^2 value of the generated Stokes beam as a function of 100 μm core size fiber length. M^2 values were calculated for a diode pump current on the Nd:YAG pump laser of 12.9 A (diamonds) and two times above the Stokes threshold (squares). 53

33. Far field pictures of generated Stokes beam output from 100 μm fiber as a function of length. Pictures were all taken at a pump energy two times above the Stokes threshold. From top left: (a) 1300 m (b) 1000 m (c) 700 m (d) 200 m. 54

34. Experimental setup for observing beam cleanup in .29 NA, 100 um graded index (GRIN) and .365 NA, 50 μm step index fiber. The 1064 nm laser light from the Nd:YAG laser served as the pump for the SRS process in the fiber. The edge filter reflected any residual pump light into a beam dump, ensuring no pump light was present when diagnostics where performed. The wedge served as a pickoff, allowing diagnostics but preventing damage to sensitive equipment. The use of 10x microscope objectives on either end of the fiber resulted in maximum coupling efficiency for the 100 μm fiber, but 16x objectives proved ideal for the 50 μm fiber due to the larger NA. 57

35. M^2 of generated Stokes beam (diagonal stripes) and transmitted pump beam (vertical stripes) for 50 μm step index fiber and 100 μm graded index (GRIN) fiber..... 58

36. Pictures of the output from the 50 μm step index fiber, allowing comparison of generated Stokes beam to transmitted pump beam. The far field pictures are with 4x zoom, while no zoom is applied for the near field. (a) Near field transmitted pump beam (b) Near field generated Stokes beam (c) Far field transmitted pump beam (d) Far field generated Stokes beam 59

37. Pictures of the output from the 100 μm graded index fiber, allowing comparison of generated Stokes beam to transmitted pump beam. The far field pictures are with 4x zoom, while no zoom is applied for the near field. (a) Near field transmitted pump beam (b) Near field generated Stokes beam (c) Far field transmitted pump beam (d) Far field generated Stokes beam 60

DEVELOPMENT OF A MULTIPLE BEAM COMBINER USING STIMULATED RAMAN SCATTERING IN MULTIMODE FIBER

1 Introduction

1.1 Chapter Overview

The purpose of this chapter is to familiarize the reader with the problem under investigation. First, a brief background describes the high level requirement for a multiple beam combiner. Second, the nonlinear optical process called stimulated Raman scattering (SRS) is explained. Third, the overarching objective of building a multiple beam combiner using SRS in multimode fiber is described. Next, four investigative questions are posed, and the relevant theory behind each is analyzed. Finally, some limitations of this experiment are discussed.

1.2 Background

The Air Force has identified a need for a high energy laser weapon placed on a tactical airframe such as the V-22, C-130, or CH-47, an effort termed the Airborne Tactical Laser (2:Sec I, 2). Two inherent issues with this program are the ability to maintain a good quality beam on target and the development of a system with a footprint small enough to fit on a tactical aircraft. The small footprint requirement could make the chemical-oxygen-iodine laser slated for use on the Airborne Laser program impractical because of the infrastructure involved. This suggests a solution might instead be found by operating several much smaller solid state lasers and combining their output to result in

the desired effect on target. Given these constraints, a multiple beam combiner using stimulated Raman scattering could be an attractive technology for the Air Force.

1.3 SRS Theory

When operating a solid state laser at high power, the beam typically suffers from aberration (4:241). In addition, if multiple aberrated solid state laser beams are only spatially overlapped, they will not produce a new beam with high beam quality. If the beams are incoherent, their intensities will simply add together. If the beams are coherent, they will interfere and the total intensity may increase. In order to physically combine the beams, one idea is that the output from each laser can be focused into its own optical fiber. These fibers can be separate input channels for a squid-like fiber combiner with many inputs and one much larger output. This physical arrangement will take care of overlapping the beams spatially and directing them toward the target. How are the effects of aberration and interference to be mitigated? The answer lies in the nonlinear optical effect known as SRS. In any atomic system, the polarization induced in the material is not proportional to the optical electric field. Rather, the polarization effect can be expressed in a Taylor series expansion as shown below (11:504):

$$P_i = \varepsilon_0 \chi_{ij} E_j + 2 d_{ijk} E_j E_k + 4 \chi_{ijkl} E_j E_k E_l + \ldots \qquad (1)$$

where E_i is the *i*th component of the instantaneous field and P_i is the *i*th component of the instantaneous polarization. χ_{ij} is the linear susceptibility, d_{ijk} is the second order susceptibility, and χ_{ijkl} is the third order susceptibility. The first order term represents the index of refraction, while the second order term is responsible for second harmonic generation, sum and difference frequency generation, and parametric amplification and

oscillation. Since glass is an isotropic material, the components of the d_{ijk} tensor are all zero, and these effects are not observed (11:508). Raman scattering arises from the third order term, and is a result of the interaction of light with the vibrational modes of the molecules in the medium causing the scattering. A photon from the pump laser is scattered by one of the molecules in the medium to a lower frequency photon, while the energy difference is transferred to the molecule by exciting it to a higher vibrational energy state (1:298). Since energy must be conserved, the following energy diagram results:

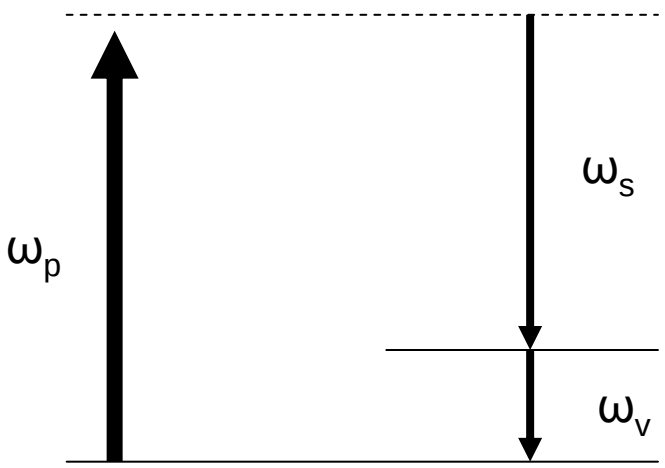

Figure 1. Energy diagram of Raman Scattering. Incoming photon at frequency ω_p is scattered by a molecule of the medium to a lower frequency Stokes photon ω_s, while the molecule makes a transition to a higher vibrational state, represented by the optical phonon at frequency ω_v.

In a previous experiment, Russell et al demonstrated SRS beam cleanup in a 300m fiber at 532 nm (9:303-316). The results of their experiment imply that after the multiple input beams are physically overlapped spatially, the resulting aberrated pump beam will be converted to a Stokes shifted output propagating in a low-order fiber mode with much better beam quality. The mechanism behind beam cleanup will be examined in Chapter 2.

1.4 Research Objectives

The objective of this experiment is to demonstrate the combination of four multimode laser beams into one beam with good beam quality through stimulated Raman scattering. This will be accomplished experimentally by starting with a single laser source, splitting the beam into the desired number of channels, recombining them using a fiber squid, enhancing the beam quality in the output fiber through the beam cleanup properties of SRS, and performing diagnostics to characterize the effect.

1.5 Investigative Questions

In preparing to perform this experiment in the lab, there are four main questions that must be examined to produce useful results. First, is there enough pump power available to meet the threshold for stimulated Raman scattering? Second, what is the energy conversion efficiency from the pump to the Stokes shifted output beam? Next, what is the beam quality of the resulting Stokes beam? Finally, does each input channel contribute to the generated Stokes beam?

1.5.1 SRS Threshold Determination

Assuming only single mode operation gives a lower bound for the amount of pump power required to meet the SRS threshold. The V parameter for a given fiber is then found through the equation below (10:279):

$$V = 2\pi \frac{a}{\lambda_0} NA \tag{1}$$

In the above equation, a is the radius of the fiber core, λ_0 is the free-space laser wavelength, and NA is the fiber's numerical aperture. From the V parameter, the mode

width parameter can be determined. Equation 2 is a fit equation, and yields the mode width parameter *w* for a graded index fiber (6:703-718):

$$w = a\left(\sqrt{\frac{2}{V}} + \frac{0.23}{V^{\frac{3}{2}}} + \frac{18.01}{V^{6}}\right) \tag{2}$$

Approximating the single mode as a Gaussian yields A_{eff}, an effective core area (1:44):

$$A_{eff} = \pi\ w^2 \tag{3}$$

The effective length, L_{eff}, is then calculated from the equation below (1:301),

$$L_{eff} = \frac{1 - e^{-\alpha L}}{\alpha} \tag{4}$$

where α is a wavelength dependent fiber attenuation constant, representing the total losses in the fiber, and L is the length of the fiber. If a Lorentzian shape is assumed for the Raman gain spectrum, the threshold power pump power, P_{th}, is then given by the equation below:

$$P_{th} = \frac{16 A_{eff}}{g_r L_{eff}} \tag{5}$$

The Raman gain coefficient, g_r, is approximately $1\times10^{-13}\ \frac{m}{W}$ for the wavelength used in this experiment (1:300). The fiber parameters used for the initial experiment are as follows: a = 50 μm, L = 2.2 km, and NA = 0.29. Using an Nd:YAG laser as a source then yields an attenuation constant of 2 dB/km or 0.461 km^{-1} for operation at 1064 nm (8:1). Inserting these values into the above equations, predicts a Raman threshold power of about 21 W for single mode operation. Because of the multimode operation of the

pump laser, and the fiber in use being a large multimode fiber, not all pump energy will propagate in the fundamental mode of the fiber. The distribution of energy throughout available fiber modes means the actual Raman threshold is likely to be much higher. This large power requirement means the laser must be used in Q-switched operation in order to produce high peak powers.

1.5.2 Energy Conversion Efficiency

The energy conversion efficiency is the ratio of output Stokes energy per pulse to coupled pump energy per pulse. The conversion efficiency is dependent on the overlap of the input pump mode with the fundamental Stokes mode (1:263). If very little pump energy is actually converted to the Stokes beam, then combining the laser beams with this method will not be an attractive choice for future work.

1.5.3 Beam Quality

In order to combine multiple input beams and demonstrate beam cleanup, the beam quality of the resulting Stokes beam must be compared to the beam quality of the transmitted pump beam below the SRS threshold. The Stokes beam tends to form a low order mode, so it should be much better than the multimode pump beam. The measure of merit used to demonstrate this is the fit parameter M^2, as used in the equation below:

$$w(z) = w_0 \sqrt{1 + \left(\frac{M^2 \lambda (z - z_0)}{\pi \ w_0^2} \right)^2} \qquad (6)$$

where *w(z)* is the beam radius as a function of distance in the *z* direction. The radius of the beam at the waist is given by w_0, λ is the wavelength of interest, and z_0 is the location on the *z* axis of the beam waist.

The beam radius is determined using the second moment method at several points along an optical rail. These data points are then used to perform a nonlinear regression fit routine in *Mathematica*, which determines the value of M^2 required. For a diffraction limited Gaussian beam, $M^2 = 1$, with worse beam quality being associated with M^2 values higher than one.

1.5.4 Input Channel Variation

The fiber squid may have a different efficiency for each input channel, and must be characterized to identify the optimum input channels. In addition, certain input channels may overlap the fundamental Stokes beam better than other channels, contributing in different degrees to the final observed beam. Differences in overlap with the fundamental Stokes beam would likely be due to where the different inputs are actually fused on the fiber squid.

1.6 Limitations

Several technical challenges exist in this experiment. The high Raman threshold, the possibility of damaging the SRS fiber while attempting to optimize coupling, and the effect of four wave mixing on the threshold of higher Stokes orders must be considered.

First, calculations of the Raman threshold for the fiber used, assuming only single mode operation, result in a needed pump power of almost 400 W. If multimode operation is allowed, which is almost certain in the large fiber core used, the Raman threshold will increase since the total *E* field in the fundamental mode will be decreased. As a result, the laser must be operated in Q-switched mode to generate the 3rd order nonlinear effect through the much larger peak powers.

The high peak power required presents a second technological challenge. While the optical components involved are built to sustain this sort of power, the fiber cladding is not. It is therefore important that the microscope objectives are of sufficient focal power to couple light directly into the core of the fiber without damaging the fiber end facets, while at the same time capturing as much incoming light as possible. In addition, precision alignment of the fiber is critical to avoid accidentally focusing incoming power into the cladding material.

The last significant technical challenge expected is the rapid onset of higher Stokes orders due to four-wave mixing. In contrast to the down-conversion of a pump photon into a lower frequency Stokes photon and a phonon discussed earlier and given by $\omega_s = \omega_p - \Omega$, the reverse process is also possible through SRS to create an anti-Stokes photon at a frequency $\omega_a = \omega_p + \Omega$ where ω_p is the pump frequency (1:343). Since $2\omega_p = \omega_a + \omega_s$, two pump photons annihilate themselves to produce anti-Stokes and Stokes photons. This process is called four-wave mixing, and can occur provided the total momentum is conserved. In the forward geometry, if the photons involved are traveling in the fundamental mode, this condition translates roughly to requiring that the indices of refraction for all frequencies concerned are the same. Because of the frequency band in question, about 100 nm, this is unlikely to allow phase matching along the entire length of the fiber. Rather, four-wave mixing can produce a seed at a given point that allows SRS to begin without having to meet the threshold.

Four-wave mixing is unlikely to significantly contribute to the first Stokes order because the corresponding anti-Stokes order does not exist. However, if the first Stokes

order is viewed as the pump, then there is already a sizeable amount of anti-Stokes energy present. This anti-Stokes seed energy, when combined with the pump energy already present, leads to the selection of a new Stokes order through four-wave mixing. In effect, the original pump and Stokes photons combine to create a new, second Stokes order with a much lower threshold requirement through the relationship $2\omega_{1s} = \omega_p + \omega_{2s}$ or equivalently, $\omega_{2s} = 2\omega_{1s} - \omega_p$. This process can go on as long as energy is available through a cascade, given by $\omega_{3s} = 2\omega_{2s} - \omega_{1s}$ and so on.

2 Literature Review

2.1 Chapter Overview

The purpose of this chapter is to familiarize the reader with recent relevant research on the topics of beam cleanup and beam combining. In the beam cleanup section, Chiang's results demonstrated that Stokes shifted beams propagate in low order fiber modes. Murray et al then explained the mechanism behind beam cleanup. Additionally, Russell et al quantified this effect in a long fiber by comparing the beam quality of the pump beam and Stokes beam. In the beam combining section, the technique of combining beams through stimulated Brillouin scattering (SBS) developed by Russell et al is reviewed.

2.2 Beam Cleanup

In 1992, Chiang examined the way fiber length impacts the evolution of the Stokes beam profile in SRS, suggesting the possibility of using SRS for beam cleanup (3:352). Chiang demonstrated that if pump beam conditions were varied, Stokes beams could be excited in a number of different fiber modes of a 30 m fiber. However, if a longer fiber length, up to 1 km, was used, the first order Stokes beam was a mixture of low order fiber modes. In addition, each of the higher Stokes orders was found to propagate in only the LP_{01} fiber mode.

In 1999, Murray et al provided two descriptions of Raman beam cleanup (7:353-371). The first description involved applying the convolution theorem to the polarization terms of the pump and Stokes beam to demonstrate that each plane-wave component of the pump mixes with every other pump component. The resulting pump intensity

spectrum was then convolved with all plane-wave components of the Stokes field. Assuming both the pump and Stokes spectrums are well behaved, the stimulated Stokes field is a smoothed version of the seeding Stokes spectrum. Murray then applied the Central Limit Theorem to show that this distribution tends toward a Gaussian.

Murray's second description of beam cleanup involved an in-depth analysis of four wave mixing between two pump components and two Stokes components. Unlike the phase matching along the forward axis using $2\omega_p = \omega_a + \omega_s$ that leads to the cascade of SRS described in Section 1.6, Murray's four wave mixing is described by $\omega_p + \omega_s = \omega_p + \omega_s$ and relies on phase matching through spatial modes. In this approach, primary Stokes components are generated along the direction of each pump component. However, secondary Stokes interactions are governed by phase-matching requirements and are generated to fill voids in the pump distribution, producing beam cleanup.

In 2002, Russell et al demonstrated that SRS in long, multi-mode fibers cleans up the beam with a dramatic improvement in beam quality, as measured by the fit parameter M^2 discussed earlier (9:315). Their results demonstrate that a poor quality 532 nm pump beam (M_p^2 = 20.7) could create a Stokes beam of much higher beam quality (M_s^2 = 2.4). This increase in beam quality represents an increase in brightness, *B*, on a given target through the equation below

$$B = \left(\frac{M_p}{M_s} \right)^4 E \qquad (7)$$

where *E* is the overall conversion efficiency to the combined Stokes orders. Since the fiber extinction coefficient is much higher at 532 nm than at 1064 nm, performing this

experiment without frequency doubling the Nd:YAG pump could reduce losses, dramatically improving the conversion efficiency, and therefore increasing brightness.

2.3 Beam Combining

If more power can be added to the aberrated pump beam through combining multiple beams, additional increases in brightness can be achieved. In 2002, Russell et al demonstrated the combination of two laser beams in a 4.4 km fiber using SBS (9:307). They determined that if the two beams are of the same frequency, coherent combining takes place. Coherent combining means both lasers collaborate to generate a common Stokes beam as soon as their sum powers reach threshold. However, if the lasers are different in frequency, incoherent combining occurs and each beam must generate its own Stokes beam, resulting in two separate thresholds. In the experiment, beam combining was investigated in terms of spatial coherence by observing interference fringes after passing the Stokes beams through a Mach-Zender interferometer.

2.4 Summary

Previous work has demonstrated the beam cleanup properties of SRS on a single pump beam at 532 nm. In addition, previous work has demonstrated beam combination using SBS. Since SRS supports both forward and backward scattering, as opposed to SBS which only supports the backward scattering geometry, SRS can be a little easier to direct. The spectral width of the SBS gain spectrum is about 10 MHz, which is much smaller than the 10 THz spectral width for SRS (1:357). The spectral widths make SRS useful for broadband lasers and SBS useful in narrow band sources. However, the Brillouin gain coefficient used to generate SBS is much larger than the Raman gain

coefficient, resulting in a higher threshold for SRS. The implication for a large core multi-mode fiber is that the pump laser must be used in pulsed operation. Finally, changing the pump to a 1064 nm source should improve efficiency, because the fiber extinction coefficient is much lower for this wavelength.

3 Observation of Beam Cleanup in 100 μm Fiber

3.1 Experimental Setup

Before multiple beam combination was considered, the first objective was to demonstrate beam cleanup in the fiber of interest. For this experiment, a 2.2 km length of 100 μm core, graded index fiber manufactured by OFS was used. The fiber had a numerical aperture (NA) of 0.29, and an attenuation coefficient of 2 dB km^{-1} at 1064 nm, the wavelength produced by the Nd:YAG laser source. The following is a diagram of the experimental setup:

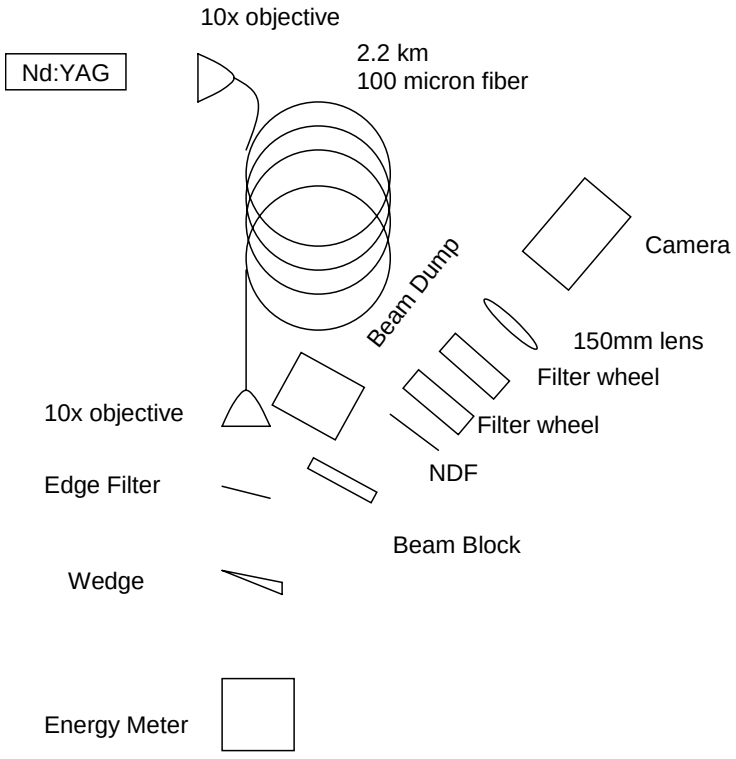

Figure 2. Experimental setup for observing beam cleanup in 100 um core fiber. The 1064 nm laser light from the Nd:YAG laser served as the pump for the SRS process in the fiber. The edge filter reflected any residual pump light into a beam dump, ensuring no pump light was present when diagnostics where performed. The wedge served as a pickoff, allowing diagnostics but preventing damage to sensitive equipment. The use of 10x microscope objectives on either end of the fiber resulted in maximum coupling efficiency.

With the edge filter in place, the beam was examined with a spectrum analyzer to ensure no pump was present. The edge filter could then be removed to evaluate the transmitted pump beam below the threshold for creation of the Stokes beam. This setup allowed pictures to be taken of the Stokes and transmitted pump beam in the far field. When the lens was removed, pictures could be taken of both beams in the near field. Since the goal of this experiment was to combine multiple laser beams for the purpose of putting high energy on a distant target, the near field refers to the collimated output of the SRS fiber, while the far field refers to the pattern produced after propagation to the target. The second moment method was used by a computer software package to find the beam center and then calculate beam diameter, which was required to determine the M^2 value for both beams.

3.2 Results

Stokes beam generation was confirmed by using a spectrum analyzer to examine the beam after the edge filter, and the results of this are shown below:

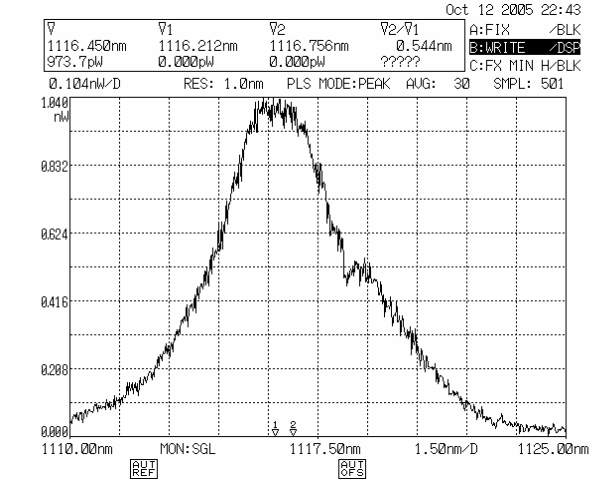

Figure 3. Spectrum demonstrating peak energy of Stokes beam occurred at 1116.5 nm.

In addition, multiple orders of Stokes beams were created as a result of the four wave mixing process described in Section 1.6. As the pump photons interact with photons from the first order Stokes beam, a second order Stokes beam is generated. This process can continue as long as power is available, and this is shown below:

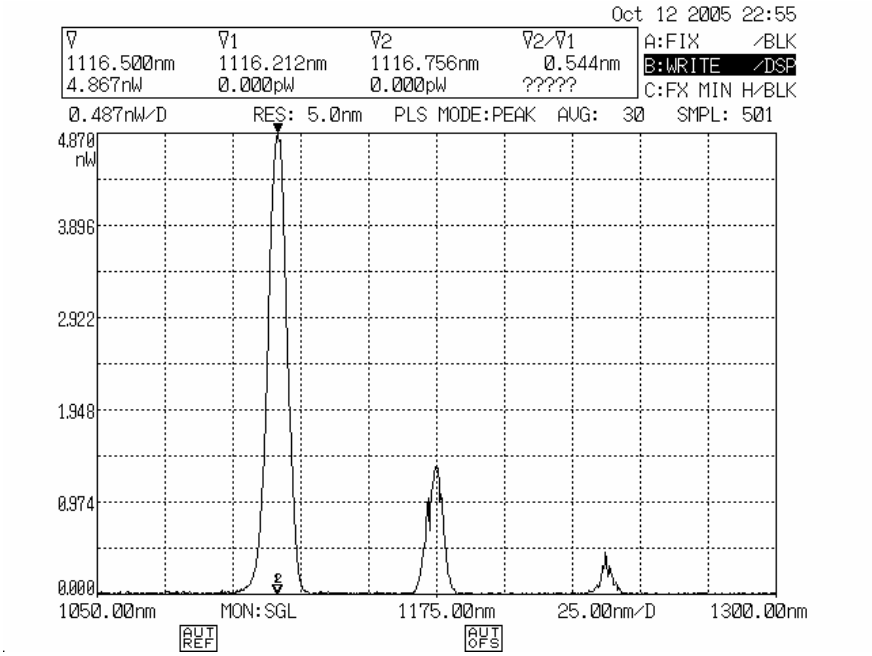

Figure 4. Spectrum of output as seen after edge filter, showing three orders of Stokes beams and confirming no pump energy is passing through the filter.

Beam cleanup was demonstrated quantitatively by comparing the Stokes beam (M^2 = 2.56) to the transmitted pump beam below the SRS threshold (M^2 = 11.04).

3.3 Summary

The M^2 value of the Stokes beam is close to the value (M^2 = 2.4) reported by Russell (9:303-316). This experiment verified that multiple orders of Stokes beams were generated. In addition to demonstrating beam cleanup occurred in this fiber, this experiment ensured the foundation was set for using the fiber squid to combine multiple pump beams.

4 Two Input Channel Fiber Squid Beam Combining and Cleanup

4.1 Experimental Setup

After demonstrating beam cleanup in the 100 μm fiber, the next objective was to demonstrate successful beam combination and cleanup using only two input channels of the fiber squid. The input fibers of the squid had a core diameter of 100 μm and an NA of 0.19, which was lower than the SRS fiber (100 μm core, 0.29 NA), but effective coupling was achieved. However, the output fiber of the squid had a core diameter of 105 μm and an NA of 0.49. The output fiber therefore had a much higher numerical aperture than the SRS fiber but only a slight increase in core size. As a result of conservation of etendue (5:1), if ideal fiber alignment was achieved, only 32% of the energy exiting the squid could be coupled into the fiber.

After inserting and aligning the squid, the microscope objectives used to couple light into the fiber had to be changed from 10x to 16x. This change was needed because the beam profile had changed after passing through the squid and was no longer the same as when the beam emerged from the laser.

The beam coming out of the Nd:YAG Lee laser at 1064 nm is unpolarized. As a result, when the beam passed through the polarization beam splitting (PBS) cube, it was evenly split, in terms of power, into two channels. One polarization, *s*, was deflected into a beam dump, while *p* polarization was allowed to pass through the cube. The PBS cube was needed because the 50/50 beam splitter that followed was only rated at 50% reflected and 50% transmitted for the *p* polarization. The goal was to provide two channels of

equal input power, and design the setup so it could easily be scaled to four channels of equal input power. The following diagram shows the experimental setup:

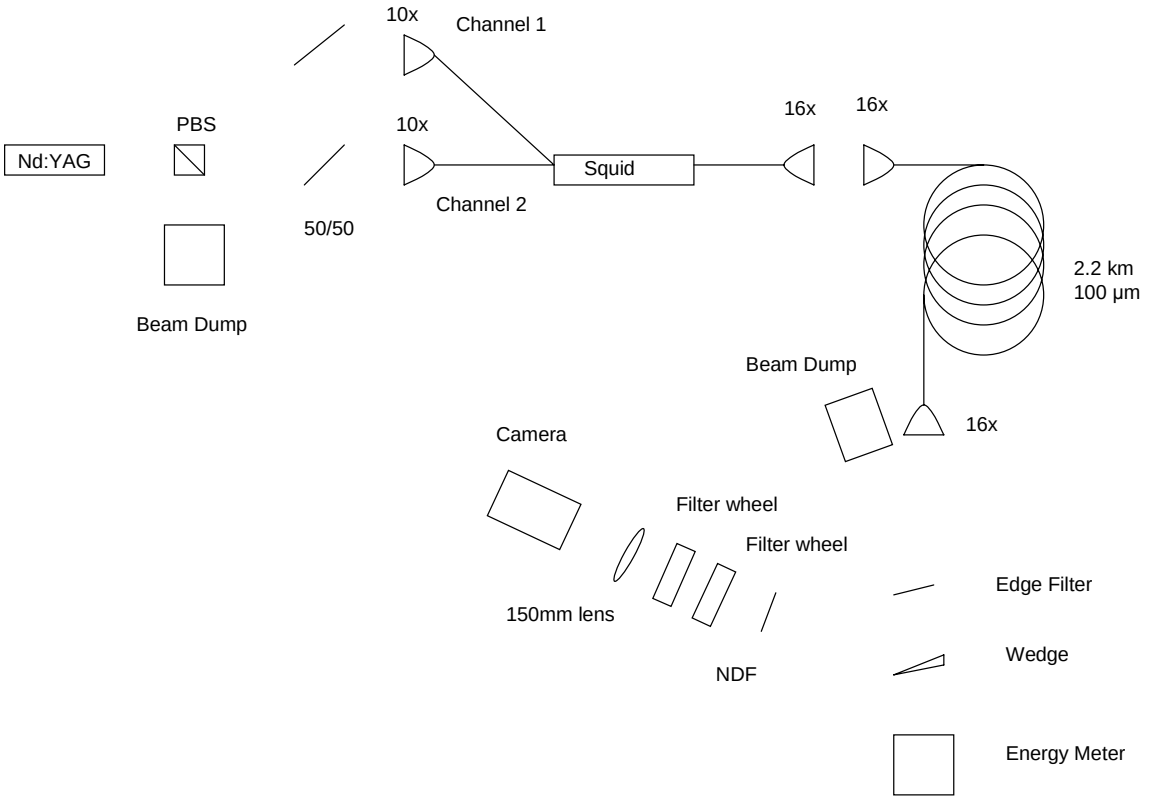

Figure 5. Experimental setup for demonstration of two channel beam combination and cleanup. The 1064 nm laser light from the Nd:YAG laser served as the pump for the SRS process in the fiber. The edge filter reflected any residual pump light into a beam dump, ensuring no pump light was present when diagnostics where performed. The wedge served as a pickoff, allowing diagnostics but preventing damage to sensitive equipment. The use of 16x microscope objectives on either end of the fiber resulted in maximum coupling efficiency.

The output channels from the 50/50 beam splitters then each passed through a 10x microscope objective and were coupled into individual inputs of the fiber squid. Using 16x microscope objectives, the output of the fiber squid was coupled into a fiber with a 100 μm core where SRS occurred. The resulting beam was composed of both undepleted 1064 nm pump power and the Stokes component at 1116.5 nm. The output of the fiber

passed through another 16x microscope objective to collimate the beam for diagnostic testing.

The pump power was separated from the Stokes power by inserting an edge filter in the beam path to reflect everything 1064 nm and below into a beam dump. The Stokes beam passed through a partially reflective (~ 4%) optical wedge, which served to pick off part of the beam. The reflection from the optical wedge was directed into the camera to take pictures of the intensity profile of the beam. Analysis software was then used to determine the beam center and diameter, using the second moment method, at different distances from the lens.

4.2 Results

Using a pulse repetition rate of 1.4 kHz and a diode pump current of 18.5 A provided enough energy to create a Stokes beam regardless of whether the channels were used independently or at the same time. When both channels were in use, about 18 μJ per pulse was measured at the output of the SRS fiber. Using a pulse width of 100 ns, 18 μJ represents a peak power of 180 W coming out of the fiber. The conversion efficiency for each possible configuration was measured, beam cleanup was demonstrated quantitatively by comparing M^2 of the Stokes beam to the M^2 of the transmitted pump, and pictures were taken of the beams in the near-field and far-field to show beam cleanup qualitatively.

4.2.1 Stokes Conversion Efficiency

The Stokes conversion efficiency was determined by dividing the Stokes energy per pulse, measured after the SRS fiber, by the pump energy per pulse after the fiber

squid with the desired channels in use. Additionally, applying the conservation of etendue (5:1) demonstrates that a maximum of 32% of the pump energy after the squid can be coupled into the SRS fiber. When conversion efficiency was calculated, the conservation of etendue was taken into account to determine how much pump energy was actually coupled into the fiber, because this problem could be fixed with an optimum fiber choice. Three cases were considered: operating channel one by itself, operating channel two by itself, or using both channels at the same time. The figure below shows how the Stokes conversion efficiency varied depending on what channels were used:

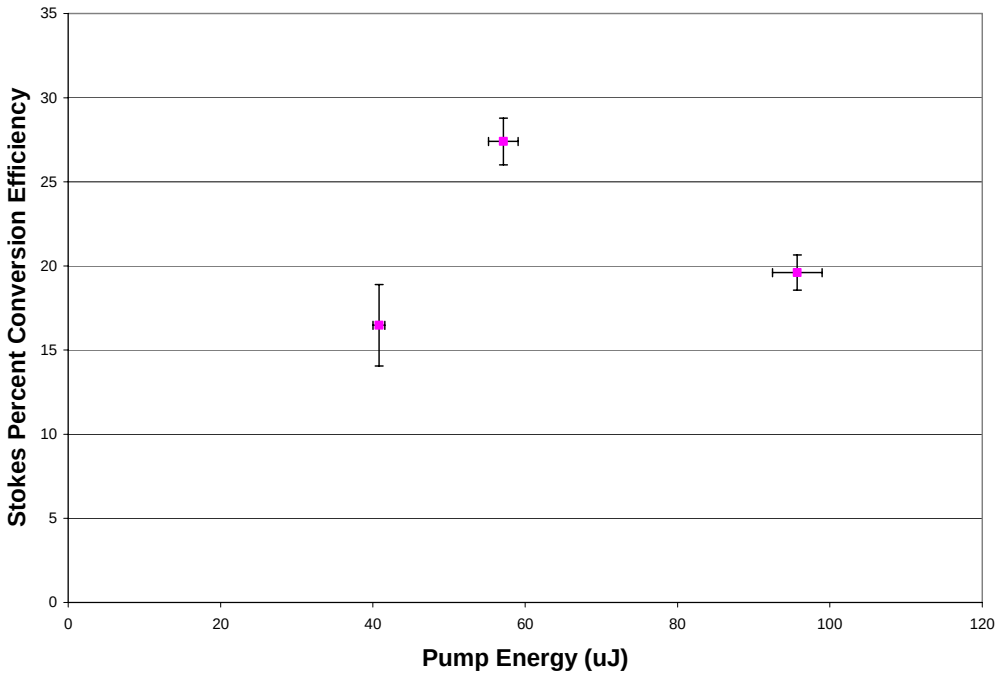

Figure 6. Percent conversion efficiency of coupled pump energy into generated Stokes energy. Pump energy of 58 µJ represents channel 1 only. Pump energy of 40 µJ represents channel 2 only. Pump energy of 95 µJ represents both channels in use simultaneously.

The higher Stokes conversion efficiency of channel 1 as compared to channel 2 could have been due to better overlap of the mode created by channel 1 with the fundamental Stokes mode of the SRS fiber. This increased overlap would then result in a

higher probability of generating Stokes energy. In addition to percent efficiency, the conversion can be looked at in terms of energy measured. The figure below shows how the energy measured after the SRS fiber compared with the measured pump energy after the squid.

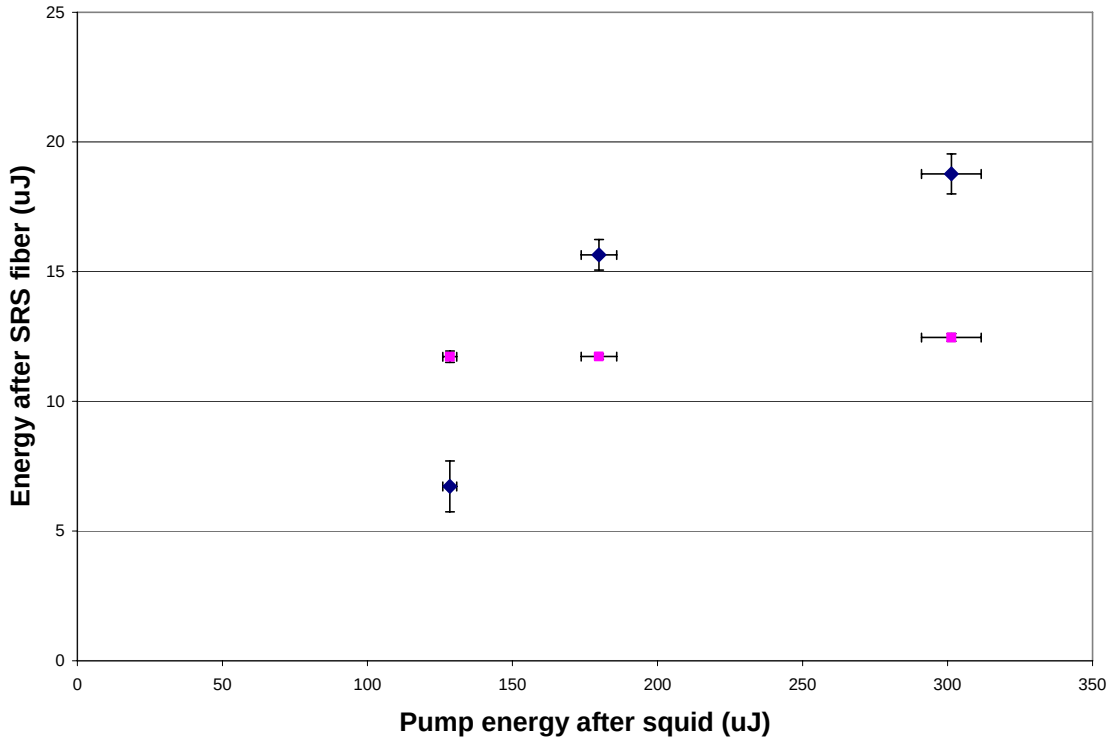

Figure 7. Measured energy after SRS fiber for different pump configurations. Measured Stokes energy after SRS fiber is represented by diamonds. Measured pump energy reflected off edge filter after SRS fiber is represented by squares. Pump energy of 180 µJ represents channel 1 only. Pump energy of 128 µJ represents channel 2 only. Pump energy of 300 µJ represents both channels in use at the same time.

The above graph demonstrated two interesting events. First, the pump energy after the SRS fiber was relatively stable, even as input pump energy was increased. This seemed to indicate the amount of energy needed to achieve threshold for the Stokes process. Second, the amount of Stokes energy when both channels were in use was less than the sum of each channel's independent use. This lower energy was unexpected,

because operation using both channels should result in even more than the sum of individual channel operations since the threshold would only have to be met once. One possible explanation for the apparent loss of energy comes from the attenuation characteristics of the fiber in use, which climbs from about 2 dB/km for the first order Stokes beam at 1116.5 nm to about 4 dB/km for at 1300 nm, as shown below:

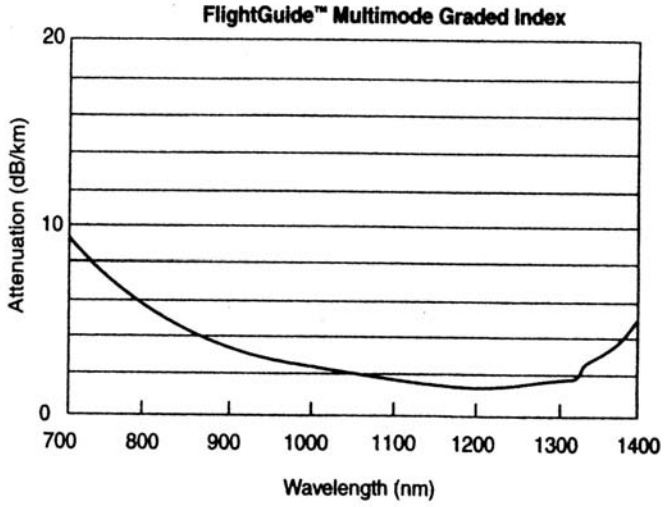

Figure 8. Attenuation data for 0.29 NA Flightguide graded index 100 μm multimode fiber used in beam combining and cleanup experiments. Data provided by ThorLabs and included when fiber was delivered.

As more energy per pulse was converted to Stokes energy, the probability of exciting higher Stokes orders increased. The energy in these higher Stokes orders was then severely attenuated by the fiber and so never measured after the fiber.

4.2.2 Beam Cleanup Demonstrated Through M^2

The camera and analysis software were used to measure the beam diameter at eleven points along the optic axis after passing through a 150 mm lens. These measurements produced a set of data points that were then fit to the equation described in Section 1.5.3 to determine the value of M^2 for the beam. After the data was taken for the

Stokes beam, the laser energy was reduced below the Stokes threshold and the edge filter was removed, allowing M^2 values to be determined for the transmitted pump. Values were calculated for the transmitted pump beam, rather than the input pump beam, because the etendue mismatch meant significant spatial filtering was occurring when the beam was coupled into the SRS fiber. As a result, the input pump beam likely had much worse beam quality than the transmitted pump beam. The following graph displays the M^2 results and demonstrates beam cleanup did occur.

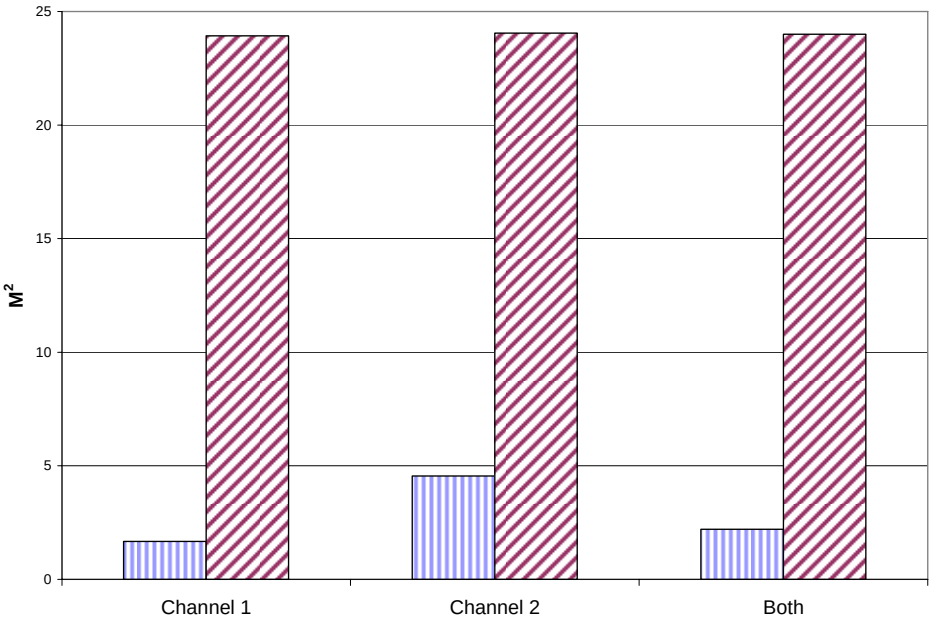

Figure 9. M^2 of the generated Stokes beam (vertical stripes) and the transmitted pump beam (diagonal stripes) depending on which channel was used.

4.2.3 Beam cleanup demonstrated through intensity profiles

Pictures were taken of the beam in the far field by photographing the beam at the waist after passing through the 150 mm lens. A smaller spot size represented better beam quality and therefore correlated with a lower M^2 value. The far field pictures were taken at 4x zoom so that features of the beam could be examined. Beam cleanup can be

demonstrated quantitatively by comparing the size of the transmitted pump beam to the generated Stokes beam. The figure below demonstrates beam cleanup by comparison of far field images of the transmitted pump and generated Stokes beams.

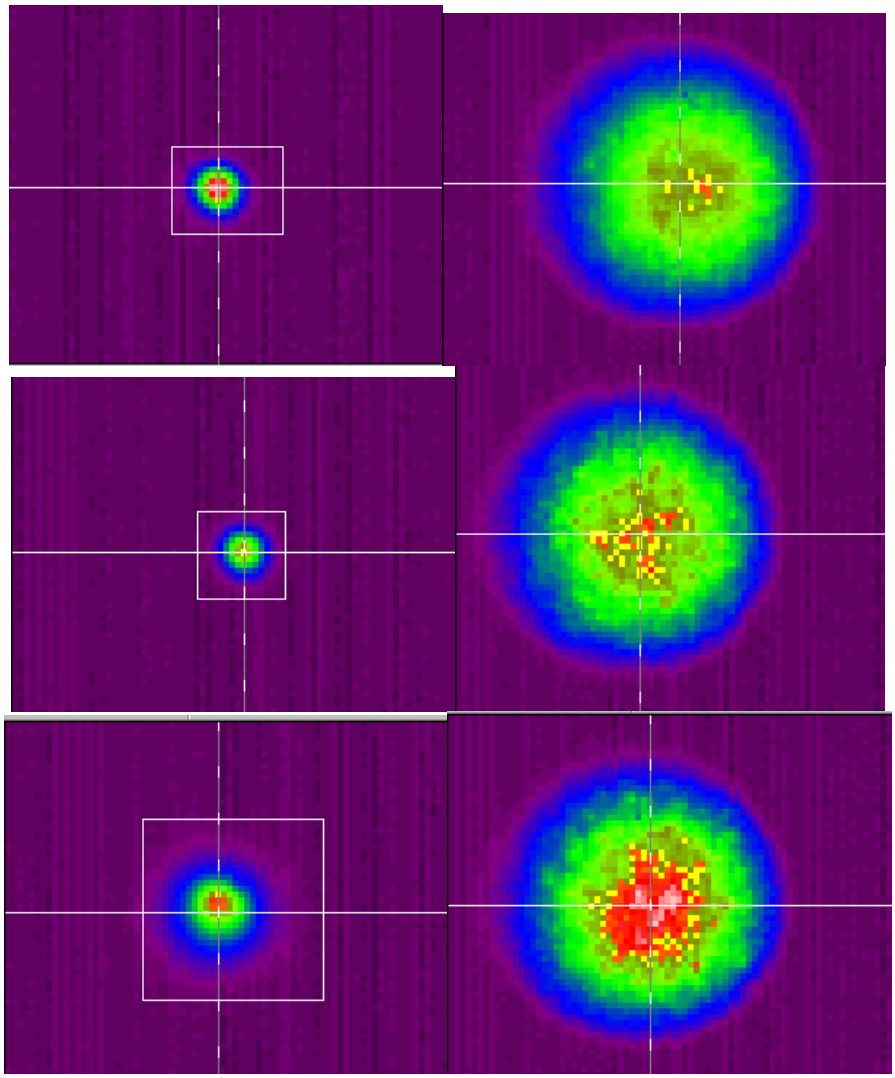

Figure 10. Far field images of generated Stokes and transmitted pump beams. The far field images of the Stokes beams are on the left, while the far field transmitted pump beams are on the right. (Top) Photographs when both channels are in operation simultaneously. (Middle) Channel 1 only. (Bottom) Channel 2 only. All pictures are at 4x zoom.

These pictures confirmed what the M^2 fit data indicated. Channel 2 only, which had the highest M^2 value, also was the largest in the far field and therefore had the worst beam quality. In addition, the Stokes beam generated by using both channels together is

not quite as small as Channel 1 only, but not nearly as big as Channel 2 only. This confirms that the Stokes beam generated when two channels are in use is affected by both channels. The lens was then removed, allowing pictures to be taken in the near field, and these are shown in the figure below.

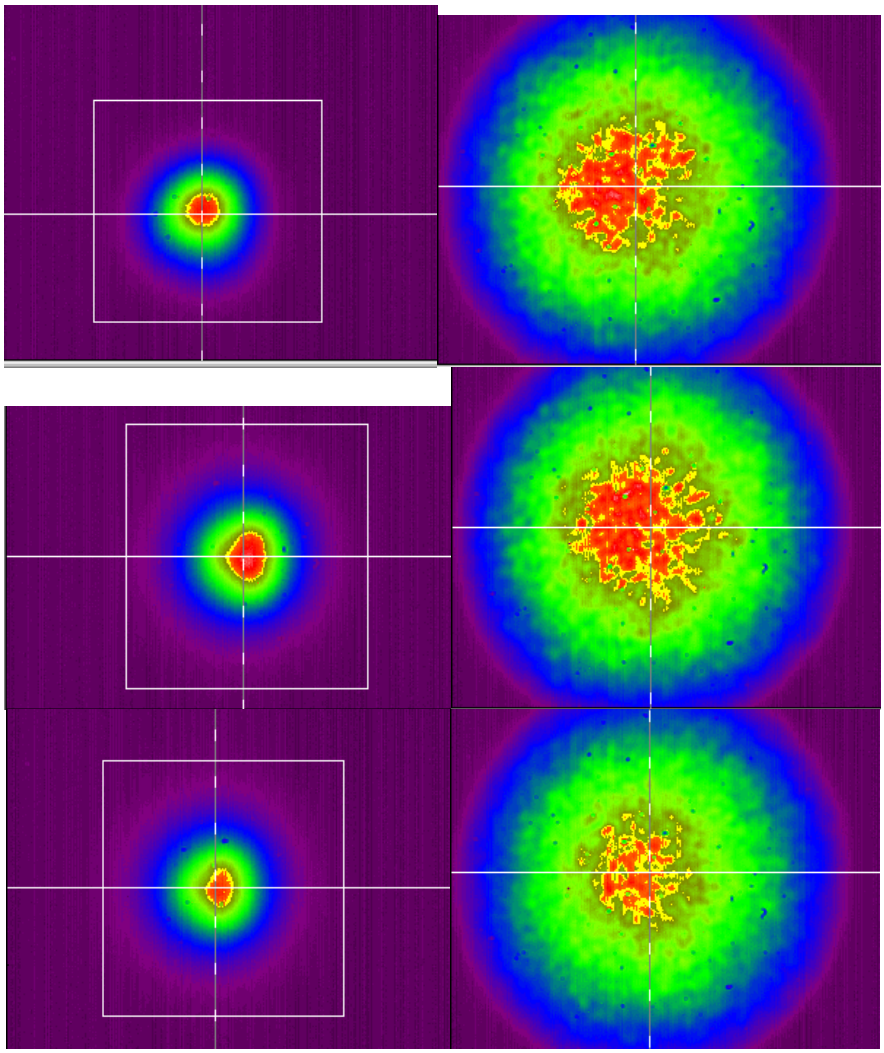

Figure 11. Near field images of generated Stokes and transmitted pump beams. The near field images of the Stokes beams are on the left, while the near field transmitted pump beams are on the right. (Top) Photographs when both channels are in operation simultaneously. (Middle) Channel 1 only. (Bottom) Channel 2 only. All pictures are with no zoom applied.

The images above demonstrate how variations in the pump beam have been corrected in the generated Stokes beam. In addition, when only one channel was used,

some small imperfections in the Stokes beam were observed. This is likely due to the way the different squid inputs are fused onto the one output, since each channel cannot exactly overlap the fundamental mode of the output fiber. As more inputs were added, the average profile will tend to be more uniform, as can be seen in the image where both channels are operating.

4.3 Summary

The results of this experiment showed that the beam produced by different input channels of the fiber squid can produce varying degrees of beam cleanup, as quantified by the different M^2 parameters. This was likely due to slight differences in the overlap of the pump beam leaving the fiber squid with the fundamental Stokes mode of the SRS fiber. Both channels contributed to the beam cleanup process, as the Stokes M^2 value increases from 1.67 to 2.20 when the poorer channel 2 ($M^2 = 4.55$) was used in addition to channel 1.

The Stokes conversion efficiency measurements supported the mode overlap argument. Channel 2, with the poorer M^2 value, had a Stokes conversion efficiency of about 16 percent, while channel 1 had a Stokes conversion efficiency of about 27 percent. At the Stokes generation threshold, regardless of which channels were used, a consistent energy of about 12 μJ per pulse was measured out of the SRS fiber. Again using a 100 ns pulse width, this energy corresponds to a peak power of about 120 W. If the mode overlap argument is correct, it is unclear why the threshold values for Stokes generation are so similar between the two channels.

In addition, it was shown that when both channels were used, the amount of Stokes energy measured was less than the sum of the Stokes energy from each channel used individually. The decrease in energy measured was attributed to the varying attenuation characteristics of the SRS fiber, which increased dramatically for longer wavelengths. As the energy per pulse increased, more energy was shifted into the higher order Stokes beams, and therefore attenuated along the length of the fiber.

5 Four Input Channel Beam Combining and Cleanup with 100 μm Fiber

5.1 Experimental Setup

After demonstrating beam cleanup in the 100 μm fiber by pumping two channels of the fiber squid, the next step was increased to four channels, proving the viability of many different pump sources. The two channel experimental setup as described in section 4.1 was revised, removing the beam dump after the PBS and inserting a half wave plate, a 50/50 beam splitter, and a mirror as shown in the figure below:

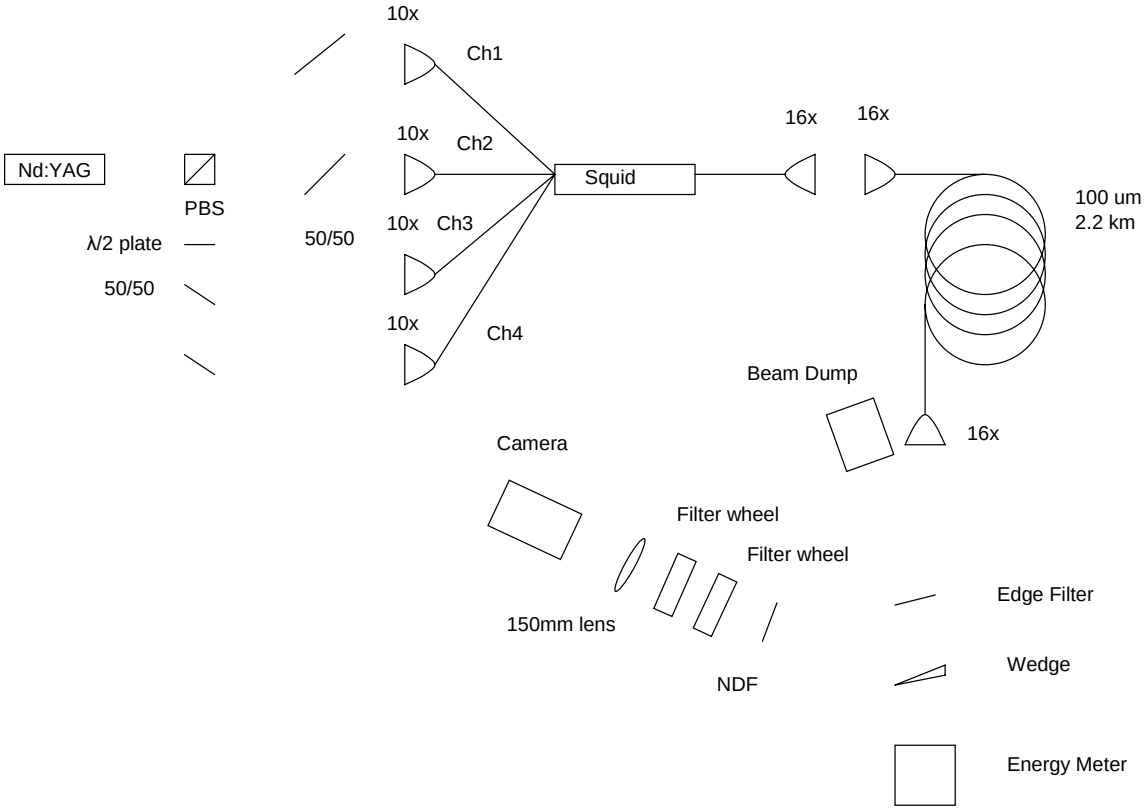

Figure 12. Experimental setup for demonstration of four channel beam combination and cleanup in 100 μm fiber. The 1064 nm laser light from the Nd:YAG laser served as the pump for the SRS process in the fiber. The edge filter reflected any residual pump light into a beam dump, ensuring no pump light was present when diagnostics where performed. The wedge served as a pickoff, allowing diagnostics but preventing damage to sensitive equipment. The use of 16x microscope objectives on either end of the fiber resulted in maximum coupling efficiency.

The half wave plate was needed because when the beam passed through the polarization beam splitting (PBS) cube, it was evenly split, in terms of power, into two channels. The beam reflected for use in channels 3 and 4, composed of *s* polarization, had to be rotated because the 50/50 beam splitter that followed was only rated at 50% reflected and 50% transmitted for the *p* polarization. The pump power and pulse repetition rate of the Nd:YAG laser did not have to be adjusted, as the energy used for these channels had simply been discarded during the two channel experiment. Upon the completion of all measurements, a one meter length of fiber was cut off the front end of the SRS fiber and the fiber spool was removed. Without changing the alignment of the input end of the fiber, this change allowed an accurate assessment of the actual amount of energy coupled into the SRS fiber as well as beam quality diagnostics of the input pump beam.

5.2 Results

First, each channel was used independently to observe Stokes generation and confirm beam cleanup occurred. Second, different combinations of two channels at a time were used to demonstrate the importance of generating Stokes energy in the fundamental mode of the SRS fiber. Third, three input channels were operated while one was blocked, with the blocked channel cycled through all channels, to ensure each channel contributed to the total Stokes beam. Next, M^2 was shown to increase with increasing pump energy. Finally, the pump-to-Stokes conversion efficiency was measured as input pump energy increased.

5.2.1 Beam Cleanup Using 4 Channels Independently

Before operating more than one channel at a time, it was verified that each input channel produced Stokes energy and cleaned up an input pump beam. The results of this experiment are displayed in the figure below:

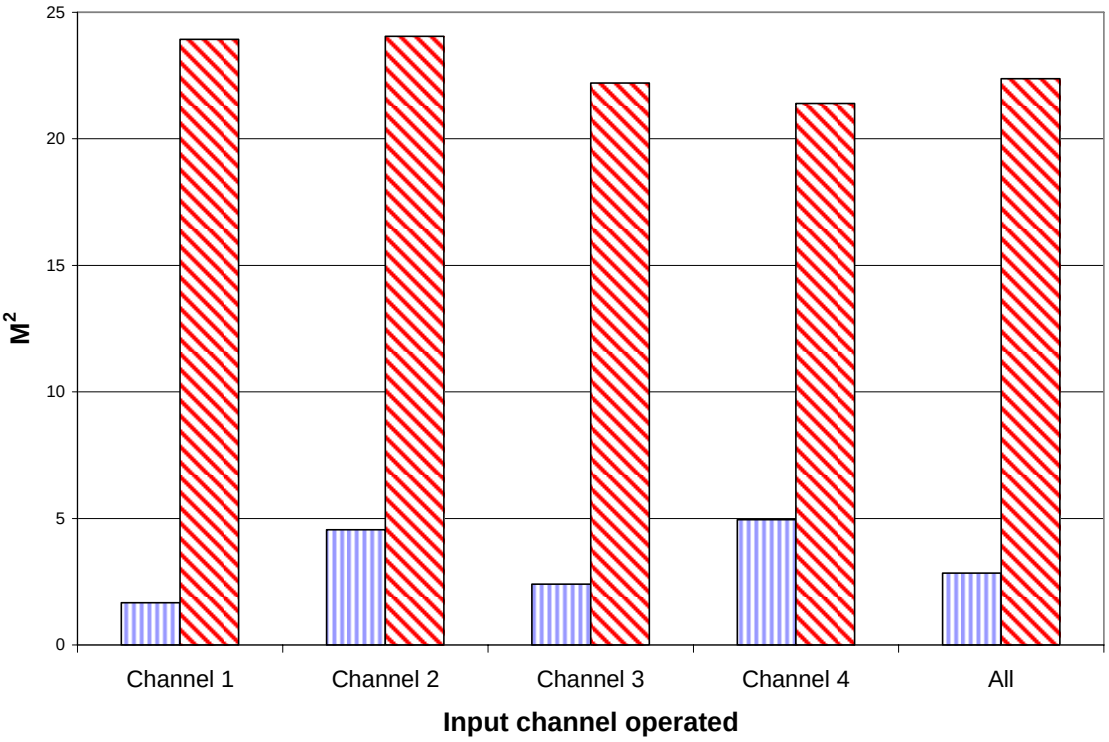

Figure 13. M^2 value of generated Stokes beam (vertical stripes) compared to transmitted pump beam (diagonal stripes) pumping input channels individually and simultaneously.

These results show that although each input channel could produce beam cleanup, some were more effective than others. Also, these results confirm the Stokes beam generated when all four channels were in use is some combination of the effects of each channel. The varying degrees of cleanup could be caused by overall poor Stokes generation, or by generation of Stokes energy in modes other than the fiber's fundamental mode. After demonstrating that input from each channel could demonstrate beam

cleanup, an experiment was performed to determine whether the poorer M^2 values were correlated with weaker Stokes generation. The results are displayed in the figure below:

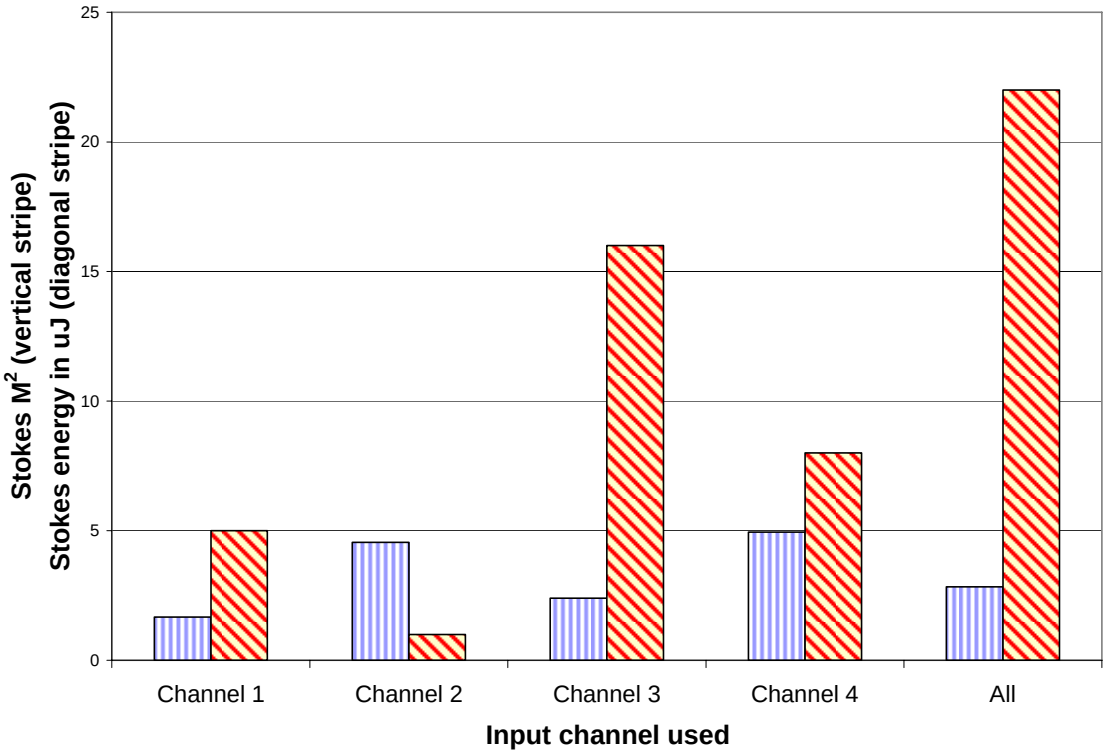

Figure 14. M^2 (vertical stripe) compared to generated Stokes energy in µJ (diagonal stripe) pumping input channels individually and simultaneously.

The results shown above confirmed that poor Stokes generation when a given input channel was pumped could not alone explain the calculated M^2 values.

5.2.2 Beam Cleanup Using Different Pairs of Input Channels

Another experiment was performed to demonstrate the importance of generating Stokes photons in the fundamental mode by determining M^2 when using different pairs of channels. The goal was to determine whether a combination of channels produced an M^2 value that was simply a weighted average of each channel's individual M^2 value, using the generated Stokes energy, *E*, as the weighting factor. After measuring the values of M^2

and E for the channel i and channel j, when each was operated by itself, the weighted average was determined through the equation below:

$$Weighted\ \ Average = \frac{\left(M^{2}{}_{i} * E_{i}\right) + \left(M^{2}{}_{j} * E_{j}\right)}{(E_{i} + E_{j})} \tag{8}$$

The experimental results are compared to the calculated weighted average values and shown below:

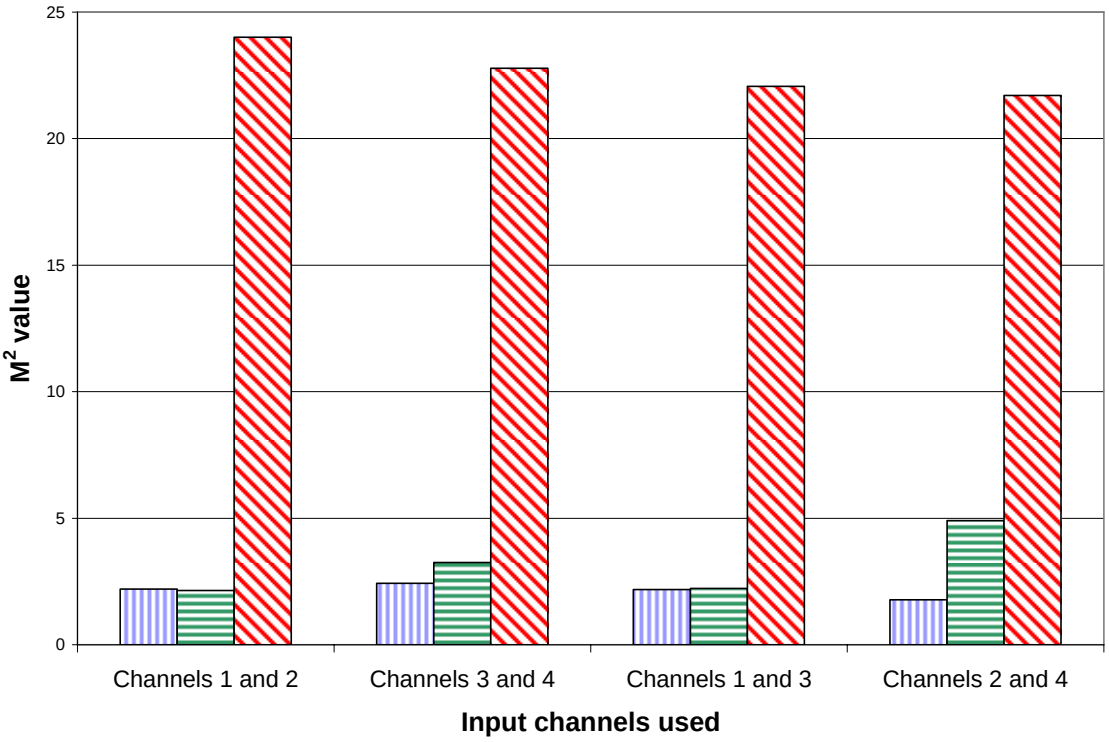

Figure 15. Measured Stokes beam M^2 (vertical stripes), calculated weighted average Stokes beam M^2 (horizontal stripes), and measured transmitted pump M^2 value (diagonal stripes) as a function of input channels used.

Two of the scenarios in the graph above (Ch1 + Ch2, Ch1 + Ch3) showed that the weighted average of individual channels was an accurate predictor of M^2 for the combination. However, the other two cases (Ch2 + Ch4, Ch3 + Ch4)demonstrated an M^2 lower than the weighted average, which suggested that the mode produced by the

combination of both input channels, rather than either channel individually, overlapped more with the fundamental Stokes mode of the SRS fiber.

5.2.3 Influence of Individual Blocked Channels on Generated Stokes Beam

The next experiment was designed to prove that each channel was contributing to the observed Stokes beam when all four channels were in use. This was accomplished by blocking each channel in turn, and observing the effect on the Stokes beam both through measuring M^2 values and examining intensity profiles of the beams. The measured M^2 values for each case are shown in the figure below:

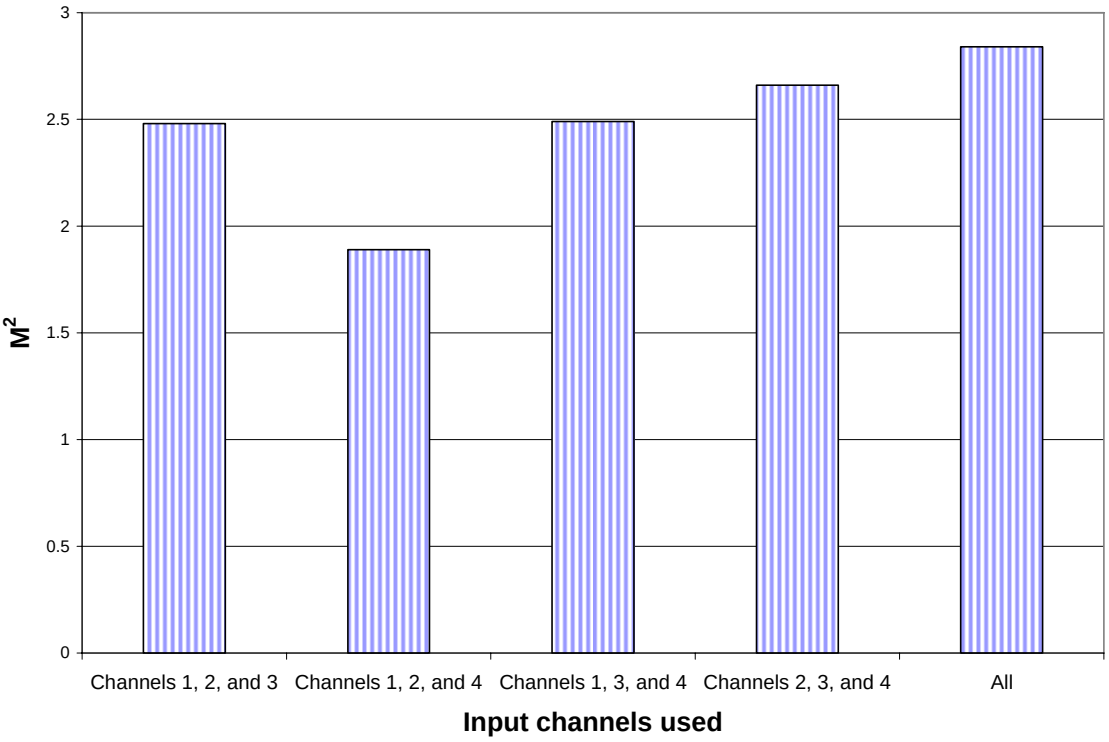

Figure 16. Impact of each input channel on M^2 value of generated Stokes beam, as determined by varying which of the four input channels were used and which was blocked.

From the graph above, it can be seen that channel 3 has a large impact on the M^2 value. This was most likely due to channel 3 generating a significant amount of Stokes

energy in modes of the Stokes beam other than the fiber's fundamental mode. This was confirmed by examining the near field pictures of the generated Stokes beam, shown below:

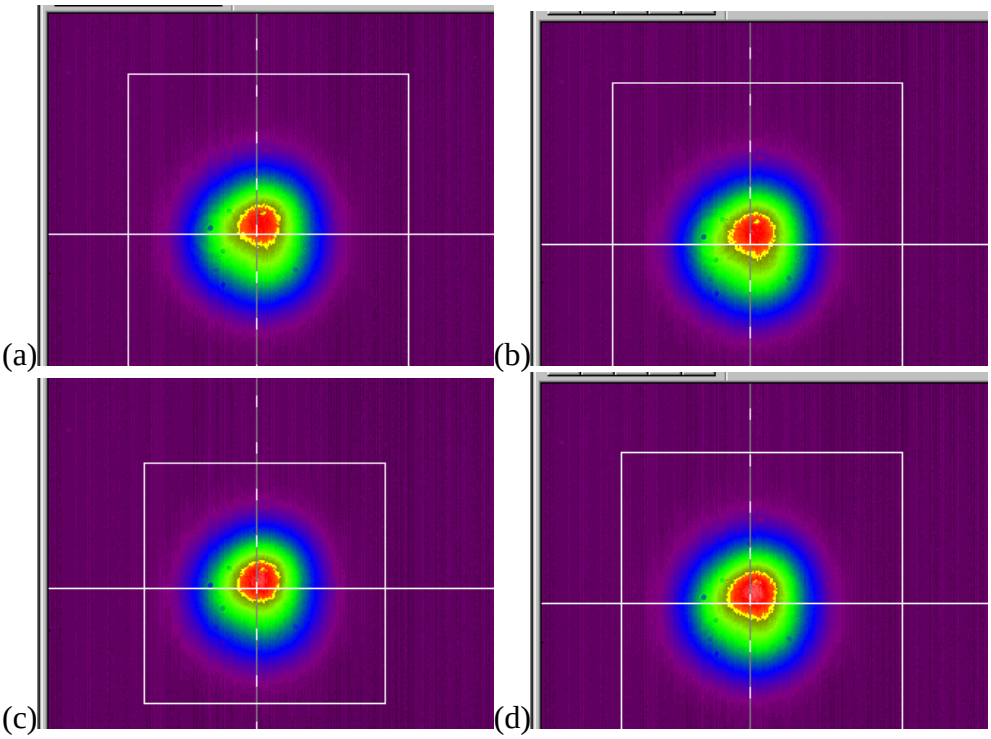

Figure 17. Intensity profile of generated Stokes beam, while blocking (a) channel 1, (b) channel two, (c) channel 3, and (d) channel 4. When channel 3 was blocked, (bottom left), the beam looks most like the fundamental mode and distortion of the central intensity region beam was somewhat reduced, becoming more circular.

5.2.4 M^2 as a Function of Coupled Pump Energy

The final experiment was to determine how M^2 of the generated Stokes beam changed when the pump energy was varied with all four channels in use. After calculating the M^2 value of the Stokes beam for each energy level, a one meter segment of the 100 μm SRS fiber was used in place of the entire 2.2 km length to accurately measure the amount of pump energy coupled into the fiber. In addition to allowing an accurate determination of energy coupled into the fiber, this change enabled an accurate

assessment of the pump beam quality immediately after any spatial filtering due to the etendue mismatch, but before higher order modes were attenuated along the fiber length. The pump M^2 proved to be very close to the earlier measurements of the pump beam quality after transmission through the entire 2.2 km length, confirming that was a reasonable process. The measured M^2 values of both beams as a function of input power are shown in the figure below:

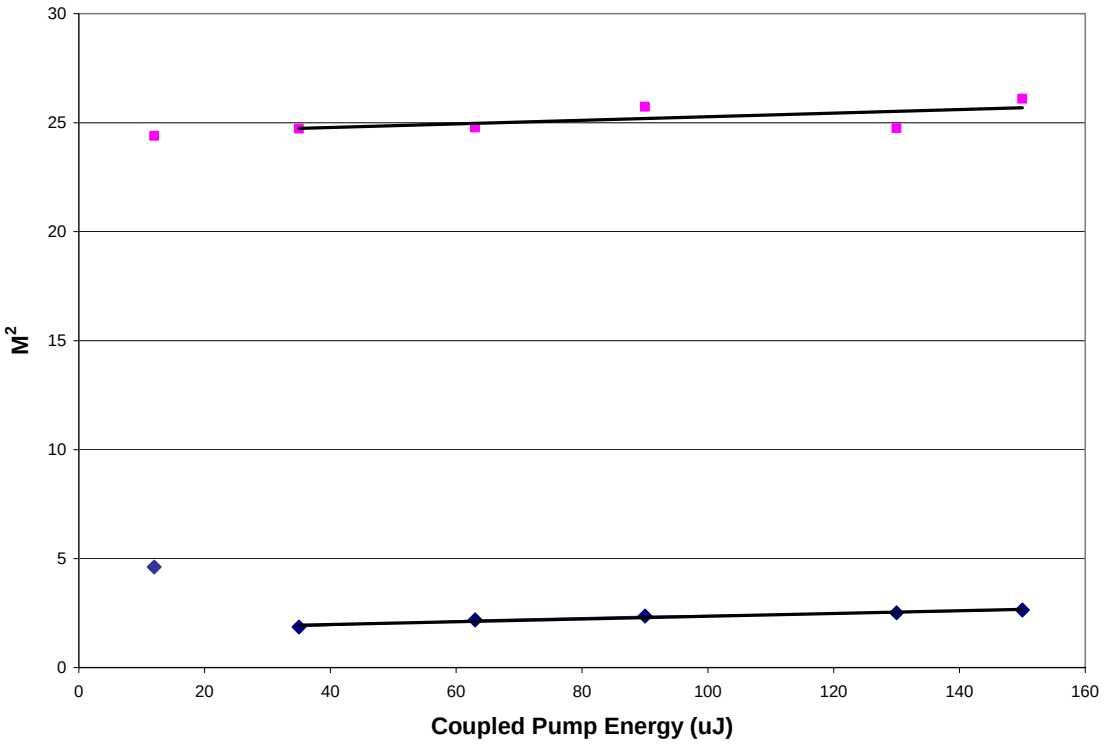

Figure 18. M^2 of generated Stokes beam (diamonds) and coupled pump beam (squares) as a function of increasing pump energy coupled into the SRS fiber.

First, these results demonstrate poorer beam cleanup around the Stokes threshold. It is not clear why this is the case, but this phenomenon was observed in multiple experiments. Next, these results demonstrate the Stokes beam quality getting slightly worse (from $M^2 = 1.86$ to $M^2 = 2.64$) as the coupled pump beam quality begins to

deteriorate. The coupled pump beam could be deteriorating because more energy is present in higher order modes at higher energies.

5.2.5 Stokes Conversion Efficiency as a Function of Power

The last experiment performed on the four channel setup was the measurement of pump-to-Stokes conversion efficiency as power was increased. A plot of the results is shown below:

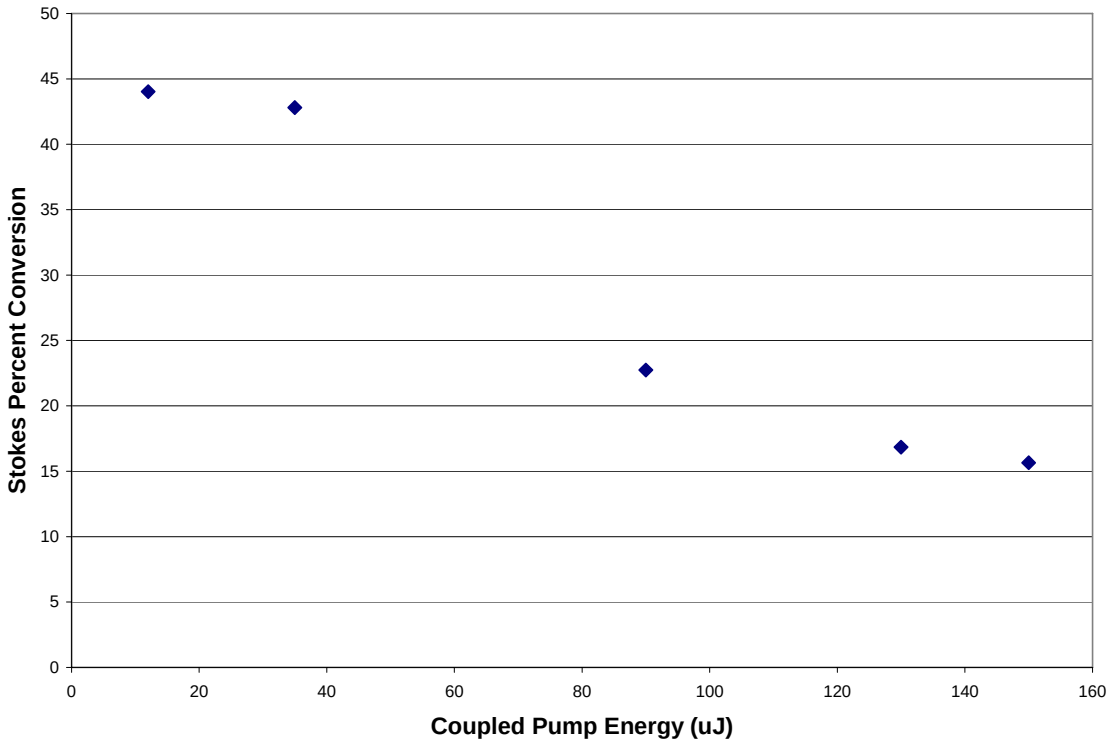

Figure 19. Percent of coupled pump energy converted into Stokes energy as a function of increasing pump energy.

The results confirmed that as the pump energy was increased, the measured Stokes conversion efficiency went down. The decrease in Stokes conversion was due to an increasing pump energy forcing more energy into higher Stokes orders, which were in turn attenuated at a much higher rate than the first order. This higher attenuation rate was

confirmed by using a spectrum analyzer to examine the output energy of the SRS fiber. Data points were taken at four different energy levels per pulse. The spectrum analyzer data showed that at high pump energies, the output spectrum was unchanged. The results confirmed that the extra pump energy was attenuated by the fiber, and the spectrum analyzer sweeps are shown below:

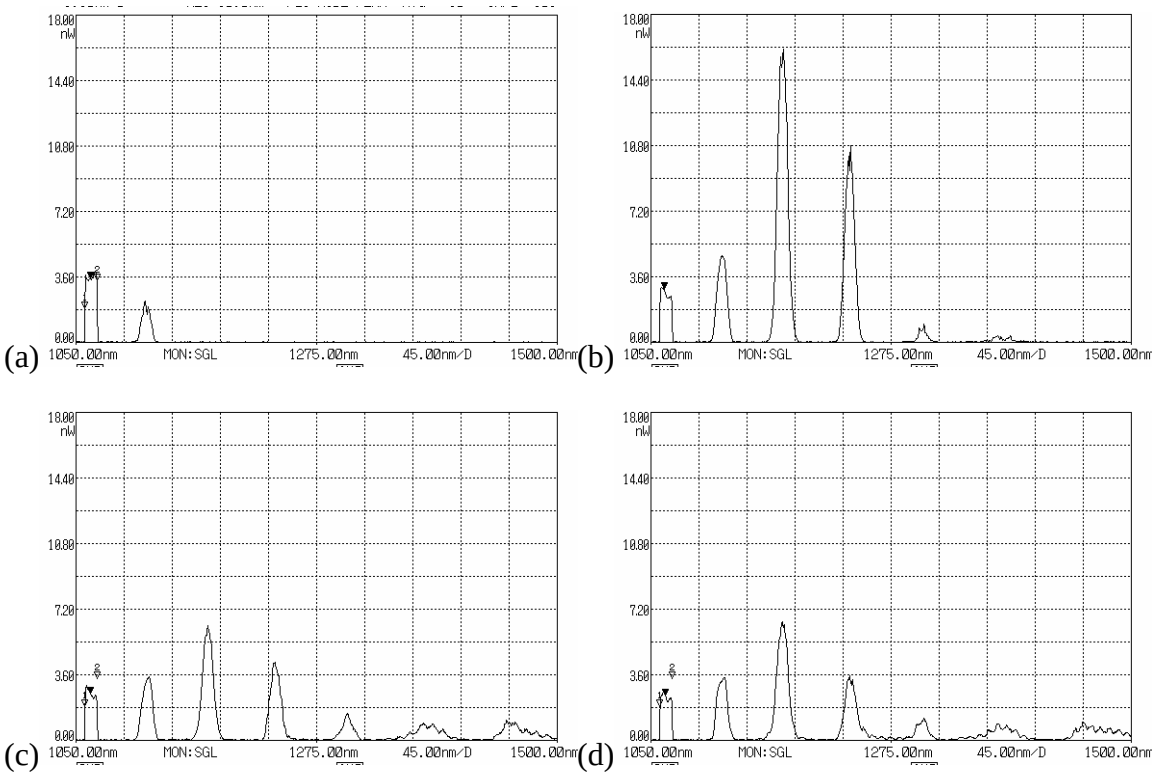

Figure 20. Spectrum analyzer sweeps from 1050 nm to 1500 nm demonstrating higher fiber attenuation of higher Stokes orders. For all graphs, wavelength is displayed on the horizontal axis, while the vertical axis is a relative intensity measurement. Graphs are for increasing pump energy coupled into the fiber: (a) At 25 µJ per pulse, the Stokes threshold has been reached. The pump beam is shown at 1064 nm and the 1st order Stokes beam is present at 1116.5 nm. (b) At 35 µJ per pulse, the effects of four-wave mixing become apparent, with three well defined Stokes orders, and hints of a fourth and fifth order. (c) At 90 µJ per pulse, the higher attenuation of the fiber at longer wavelength is shown, as the fifth and sixth Stokes orders are generated, but remain very low in intensity. (d) At 150 µJ per pulse, the relative intensities of the higher Stokes orders are almost unchanged from the sweep shown in (c), confirming the extra energy has been lost in the fiber.

To verify that the increased pump energy was not simply converted to a higher Stokes order outside the measured wavelength range, the total energy output from the

SRS fiber was compared to the diode pump current of for the Nd:YAG laser. The results of this measurement are shown below:

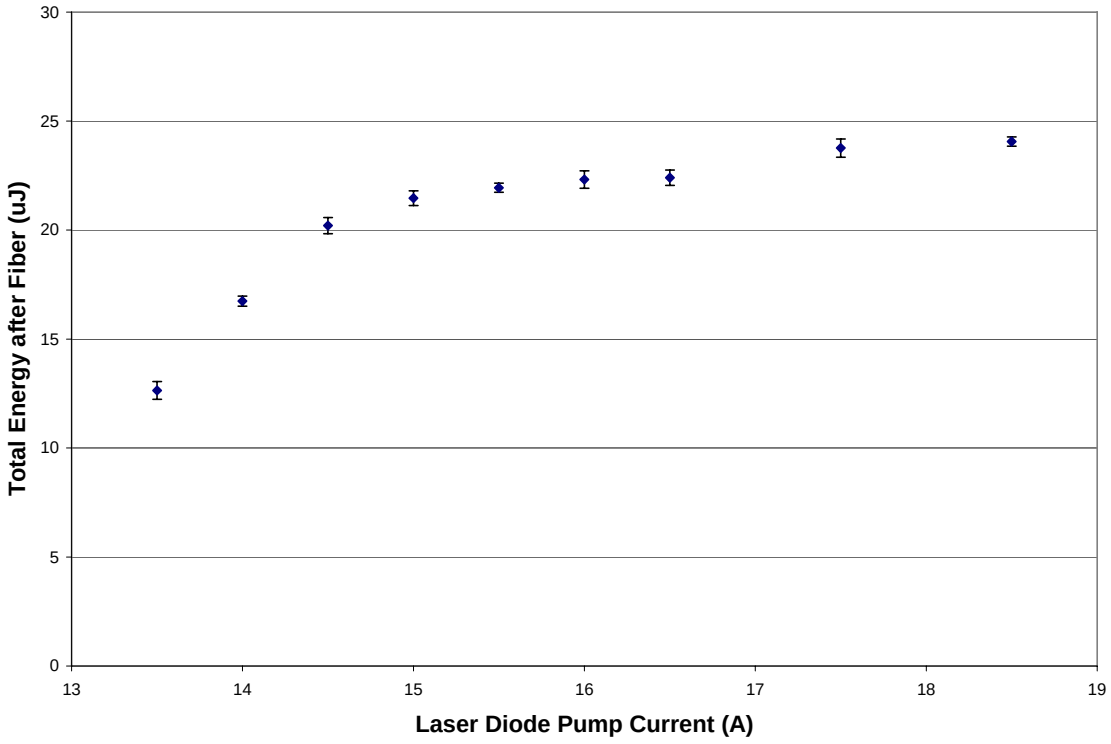

Figure 21. Generated Stokes energy in the 100 μm fiber as a function of increasing Nd:YAG laser diode pump current.

The graph above demonstrated that as diode pump current, and therefore pump energy, increased, the total amount of energy measured leaving the fiber was approaching a constant value. This reinforces the notion that the fiber had a much higher attenuation for longer wavelengths, and above a certain point, increasing pump energy was deposited into higher Stokes orders, then lost and converted to heat in the fiber.

5.3 Summary

The results of this experiment demonstrated that four separate pump beams could be combined into one Stokes beam of good beam quality. An optimum value of M^2 was

identified with $M^2 = 1.86$ at 35 μJ of pump energy. The contribution of each pump input channel was verified by blocking one channel at a time and observing the effect on the Stokes beam quality with input pump energy remaining constant. At the energy level chosen, beam quality was the worst ($M^2 = 2.84$) when all channels were used. However, the M^2 values ranged from 1.89 to 2.66 depending on which individual channel was blocked, demonstrating that each pump beam was contributing.

For two channels, the generated Stokes beam quality could sometimes be predicted by a weighted average of both the M^2 values of each channel individually, but in other cases the weighted average was not a good predictor of beam quality. This inconsistency was explained by recalling the importance of the overlap of the superimposed pump beams with the fundamental Stokes mode of the SRS fiber.

In addition, once above the Stokes threshold, M^2 was shown to increase from an optimum value ($M^2 = 1.86$) to the worst value ($M^2 = 2.64$) with increasing pump energy. The lower quality Stokes beam was explained by higher energy pump beams having more energy in higher order modes, and therefore the value of the overlap integral grows for modes other than the fundamental mode.

Finally, the pump-to-Stokes conversion efficiency decreased from a high of 44% to a low of 16% as input pump energy increased. This was determined to be due to the higher attenuation characteristics of the SRS fiber at longer wavelengths. Above a certain wavelength, excess pump energy was absorbed by the fiber rather than contributed to higher Stokes orders. The increased absorption meant that very little additional Stokes energy was observed as the pump energy was increased, thus the overall conversion efficiency was decreased.

6 Four Input Channel Beam Combining and Cleanup with 200 μm Fiber

6.1 Experimental Setup

After demonstrating beam combination and cleanup in the 100 μm fiber using four input channels of the fiber squid, the next variation was to modify the experimental setup described in section 5.1 by replacing the 100 μm fiber spool with a 2.5 km spool of 200 μm core size, .275 NA, graded index fiber. The larger core size of the 200 μm fiber, but similar NA, meant that more of the light emerging from the fiber squid could be coupled into the fiber. The revised experimental setup is shown in the figure below:

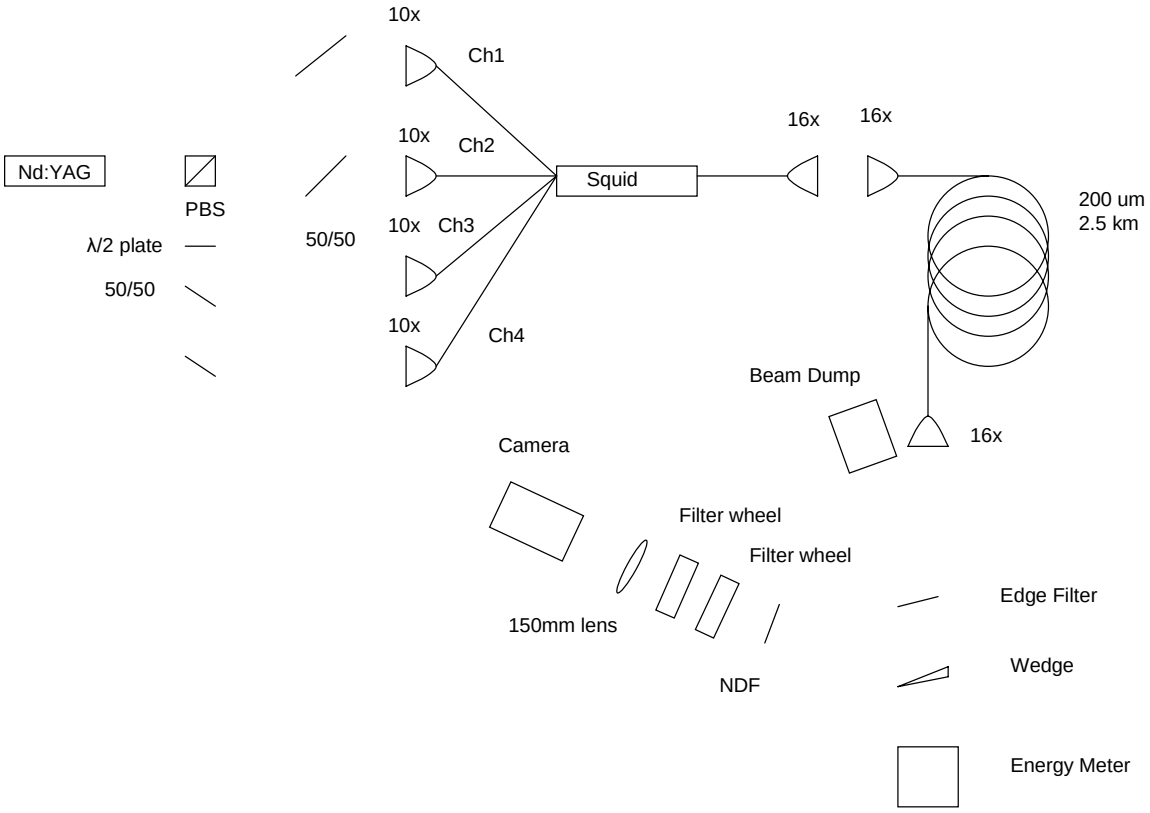

Figure 22. Experimental setup for demonstration of four channel beam combination and cleanup. The 1064 nm laser light from the Nd:YAG laser served as the pump for the SRS process in the fiber. The edge filter reflected any residual pump light into a beam dump, ensuring no pump light was present when diagnostics where performed. The wedge served as a pickoff, allowing diagnostics but preventing damage to sensitive equipment. The use of 16x microscope objectives on either end of the fiber resulted in maximum coupling efficiency.

After all SRS measurements were performed, a one meter length was cut off the fiber spool, without changing the input alignment, to determine the total energy coupled into the fiber at each laser pump power setting. This enabled an exact measurement of Stokes conversion efficiency in the fiber.

6.2 Results

First, M^2 was shown to increase with increasing pump energy. Next, the pump-to-Stokes conversion efficiency was measured as input pump energy increased. Finally, a comparison was performed between the 100 μm fiber and the 200 μm fiber.

6.2.1 M^2 as a Function of Coupled Pump Energy

The first experiment was to determine how M^2 of the generated Stokes beam changed when the pump energy was varied with all four channels in use. After calculating the M^2 value of the Stokes beam for each energy level, a 1 m segment of the 200 μm SRS fiber was used in place of the entire 2.5 km length. This change allowed an accurate determination of energy coupled into the fiber at every laser pump power.

First, these results demonstrated poor beam cleanup around the Stokes threshold. It is not clear why this is the case, but this phenomenon was verified multiple times and confirmed what was observed in experiments with the 100 μm fiber. Next, this experiment produced an optimum M^2 value of 1.4 at a pump energy 139 μJ. Additionally, these results showed the Stokes beam quality getting slightly worse as pump energy increased while no deterioration was observed in the coupled pump beam quality. The measured M^2 values of both beams as a function of input power are shown in the figure at the top of the next page.

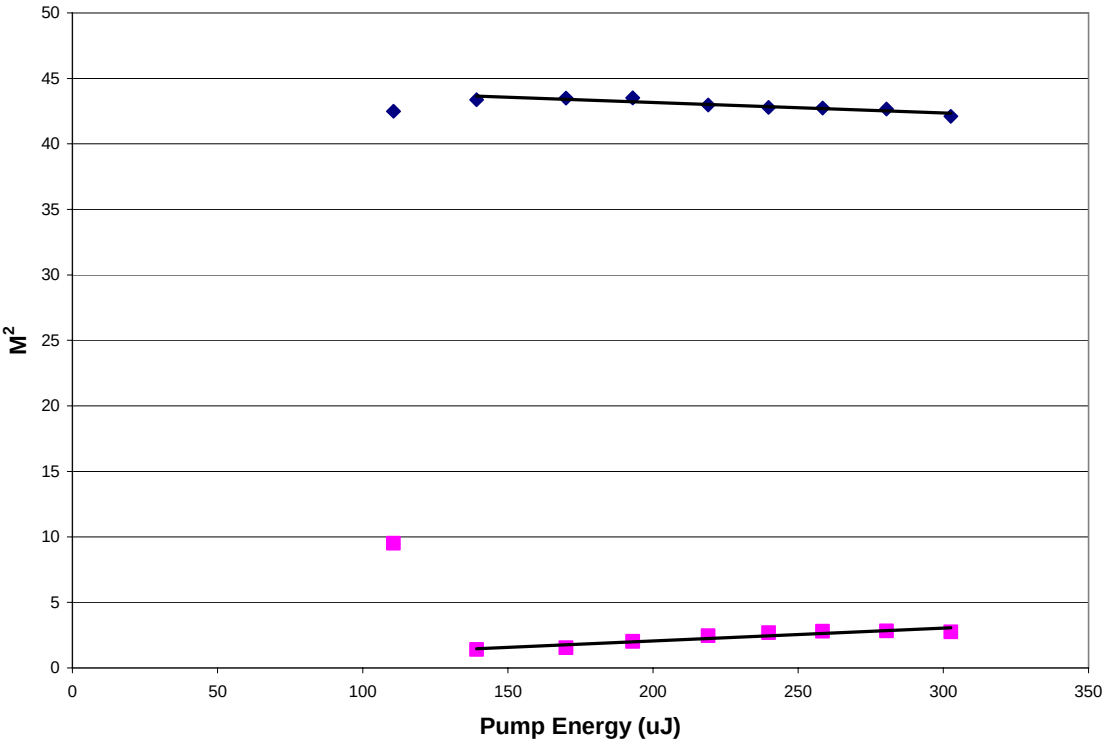

Figure 23. M^2 of generated Stokes beam (squares) and coupled pump beam (diamonds) as a function of increasing pump energy coupled into the 200 µm SRS fiber.

The deterioration of the Stokes beam was due to higher energy densities exciting modes other than the fundamental mode of the fiber. This idea was supported by the far field pictures of the generated Stokes beam, taken at various pump energy levels, shown at the top of the next page.

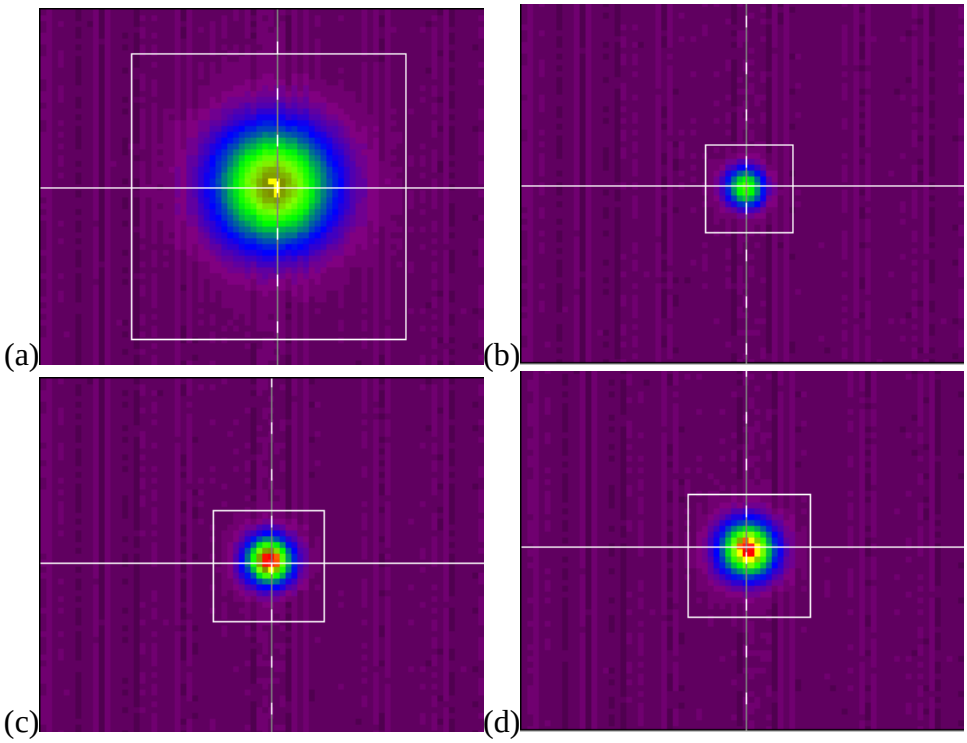

Figure 24. Effect of input pump energy on beam quality of Stokes beam generated in 200 µm fiber as shown by far field pictures of the beam. (a) 110 µJ, M^2 = 9.51 right at the Stokes threshold (b) 139 µJ, M^2 = 1.40 slightly above Stokes threshold (c) 193 µJ, M^2 = 2.02 (d) 303 µJ, M2 = 2.75

6.2.2 Stokes Conversion Efficiency as a Function of Power

The next experiment performed on the four channel setup was the measurement of pump-to-Stokes conversion efficiency as power was increased. A plot of the results is shown at the top of the next page.

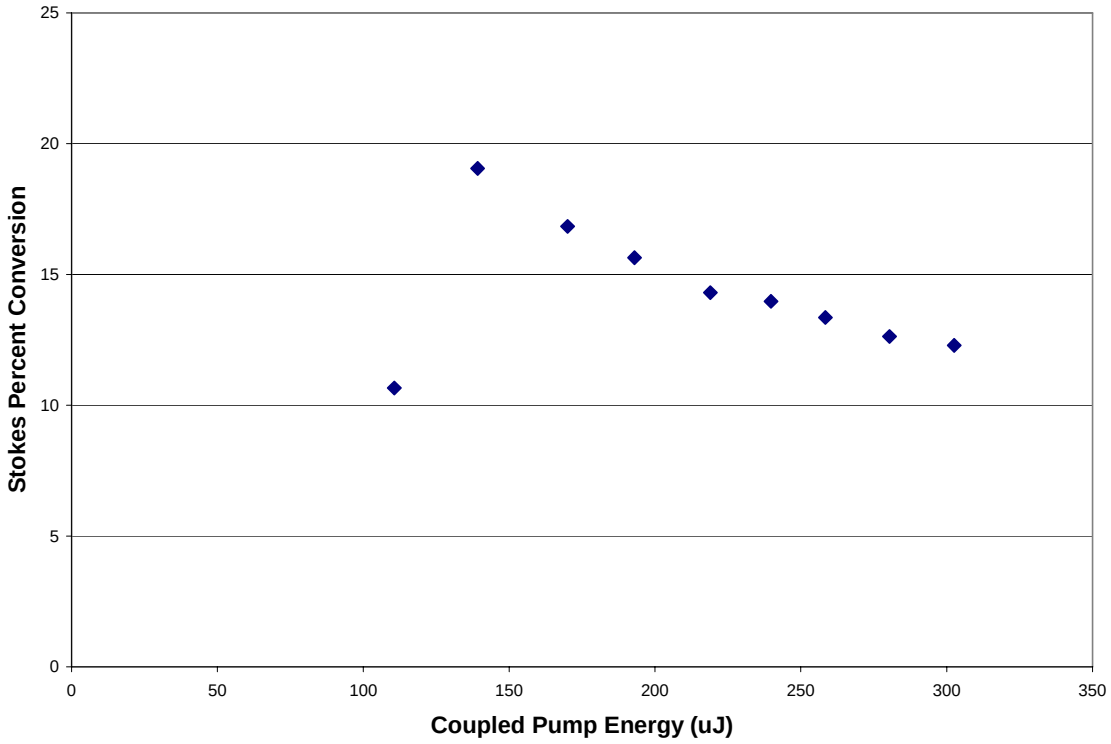

Figure 25. Percent of coupled pump energy converted into Stokes energy as a function of increasing pump energy in the 200 μm SRS fiber.

The results confirmed that as the pump energy was increased, the measured Stokes conversion efficiency went down. The decrease in Stokes conversion was due to an increasing pump energy forcing more energy into higher Stokes orders, which were in term attenuated at a much higher rate than the first order. This higher attenuation rate was confirmed by using a spectrum analyzer to examine the output energy of the SRS fiber, and the results are shown at the top of the next page.

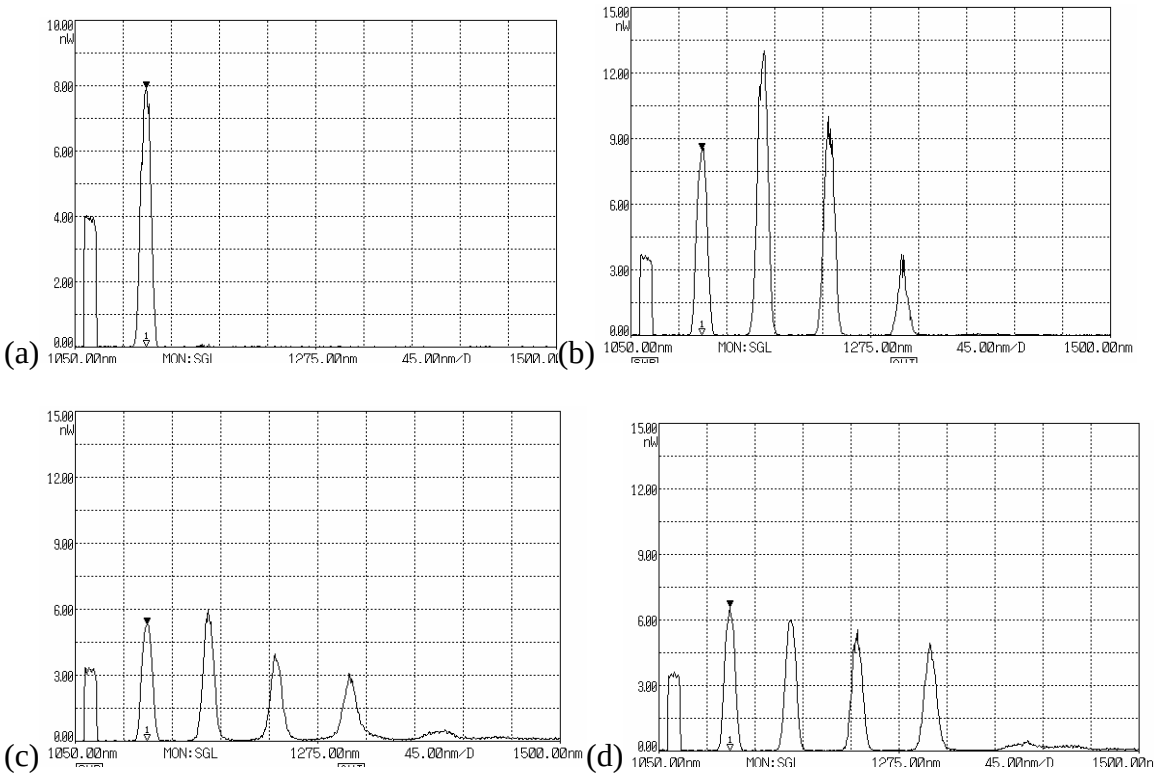

Figure 26. Spectrum analyzer sweeps from 1050 nm to 1500 nm demonstrating higher fiber attenuation of higher Stokes orders. For all graphs, wavelength is displayed on the horizontal axis, while the vertical axis is a relative intensity measurement. Graphs are for increasing pump energy coupled into the fiber: (a) At 110 µJ per pulse, the Stokes threshold has been reached. The pump beam is shown at 1064 nm and the 1st order Stokes beam is present at 1116.5 nm. (b) At 140 µJ per pulse, the effects of four-wave mixing become apparent, with four well defined Stokes orders. (c) At 170 µJ per pulse, the higher attenuation of the fiber at longer wavelength is shown, as the fifth Stokes order is generated, but remains very low in intensity. (d) At 300 µJ per pulse, the relative intensities of the higher Stokes orders are very similar to the sweep shown in (c), confirming the extra energy has been lost in the fiber.

To verify that the increased pump energy was not simply converted to a higher Stokes order outside the measured wavelength range, the total energy output from the SRS fiber was compared to the amount of pump energy coupled into the fiber, and the results are shown at the top of the next page.

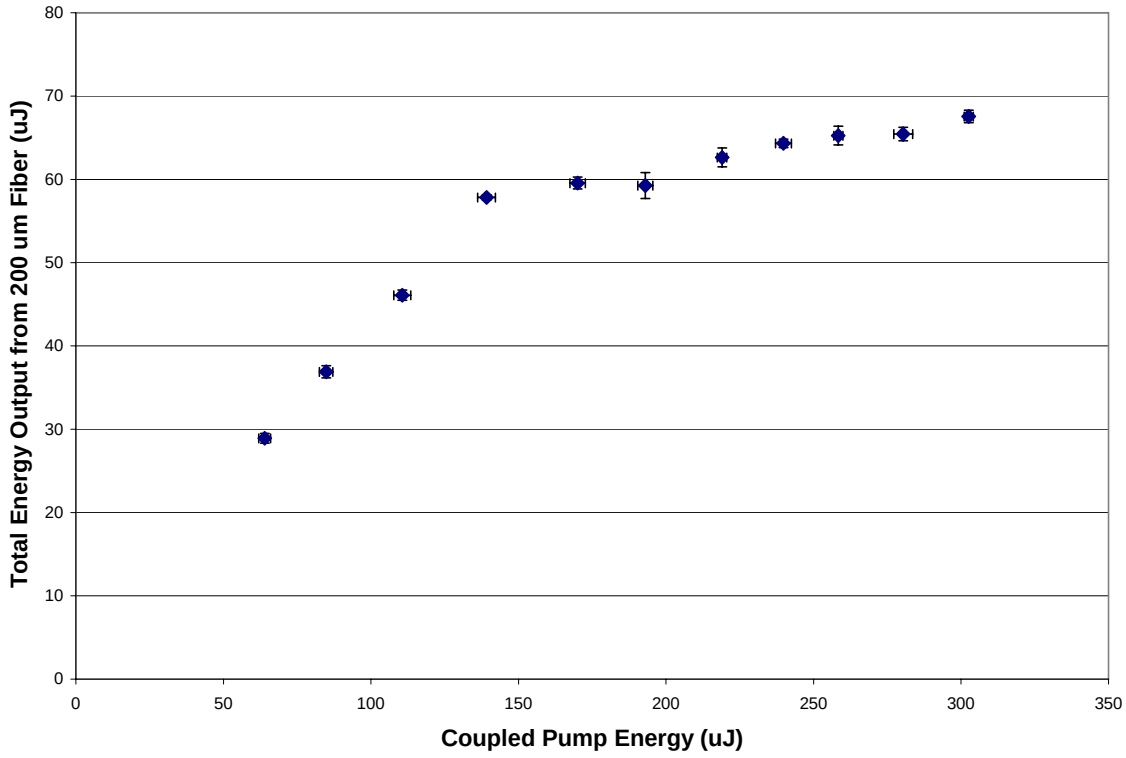

Figure 27. Total energy output from 200 μm fiber as a function of increasing pump energy coupled into the fiber.

The graph above demonstrated that as more pump energy was coupled into the fiber, the total amount of energy measured leaving the fiber was changing very little. This reinforces the notion that the fiber had a much higher attenuation for longer wavelengths, and above a certain point, increasing pump energy was coupled into higher Stokes orders, then lost and converted to heat in the fiber.

6.2.3 Performance Comparison to 100 μm Fiber

The performance of the 200 μm fiber was compared to the 100 μm fiber in terms of generated Stokes beam quality, Stokes conversion efficiency, and total amount of Stokes energy output. Limitations on coupling efficiency and available power meant that the data points for both fibers only overlapped in a small region, but overall trends were

discovered. The generated Stokes beam quality as a function of power is shown below for both fibers:

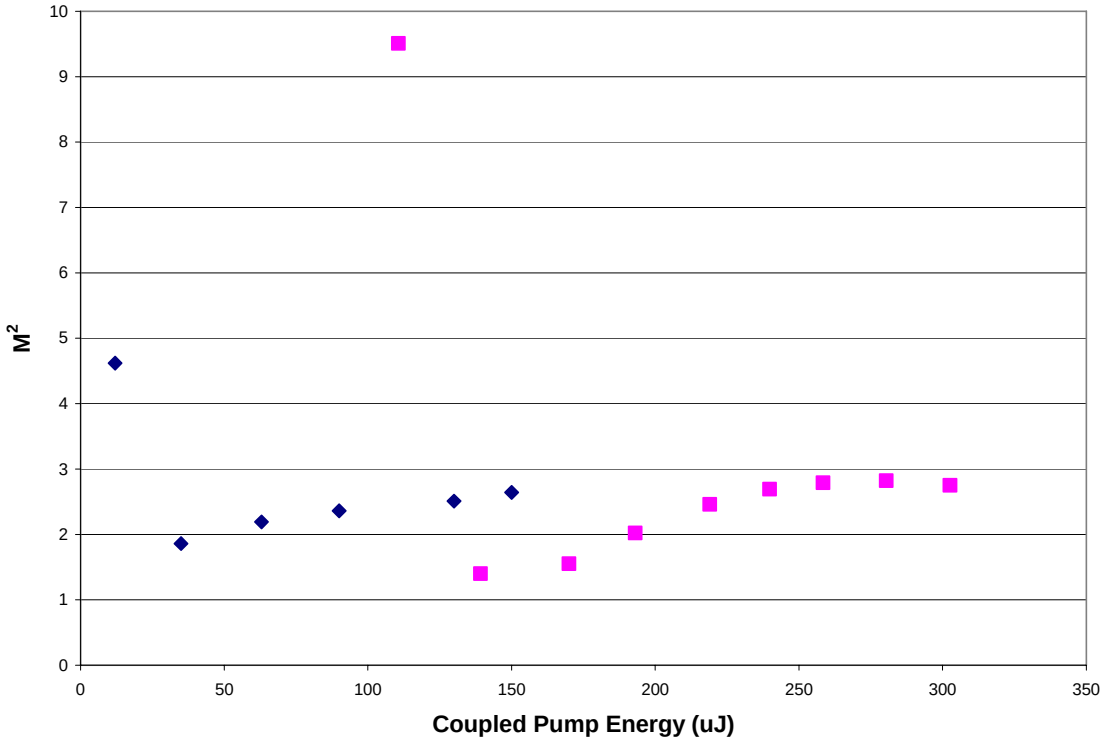

Figure 28. M^2 of generated Stokes beam from 100 μm fiber (diamonds) and 200 μm fiber (squares) as a function of increasing pump energy coupled into the fiber.

The graph above demonstrated that the generated Stokes beam quality was poor around the Stokes threshold, then improved to an optimum value, and began to deteriorate as power was increased. As explained in section 1.5.1, the higher threshold energy of the 200 μm fiber was directly due to the larger effective area since the fibers had very similar effective lengths. Because of the larger cross section, if the same amount of energy is coupled into each fiber, the energy density will be four times higher in the 100 μm fiber. As a result, the high peak powers required for SRS are more easily obtained in the 100 μm fiber.

The Stokes conversion efficiency was measured at different powers for both fibers, and the results are shown below:

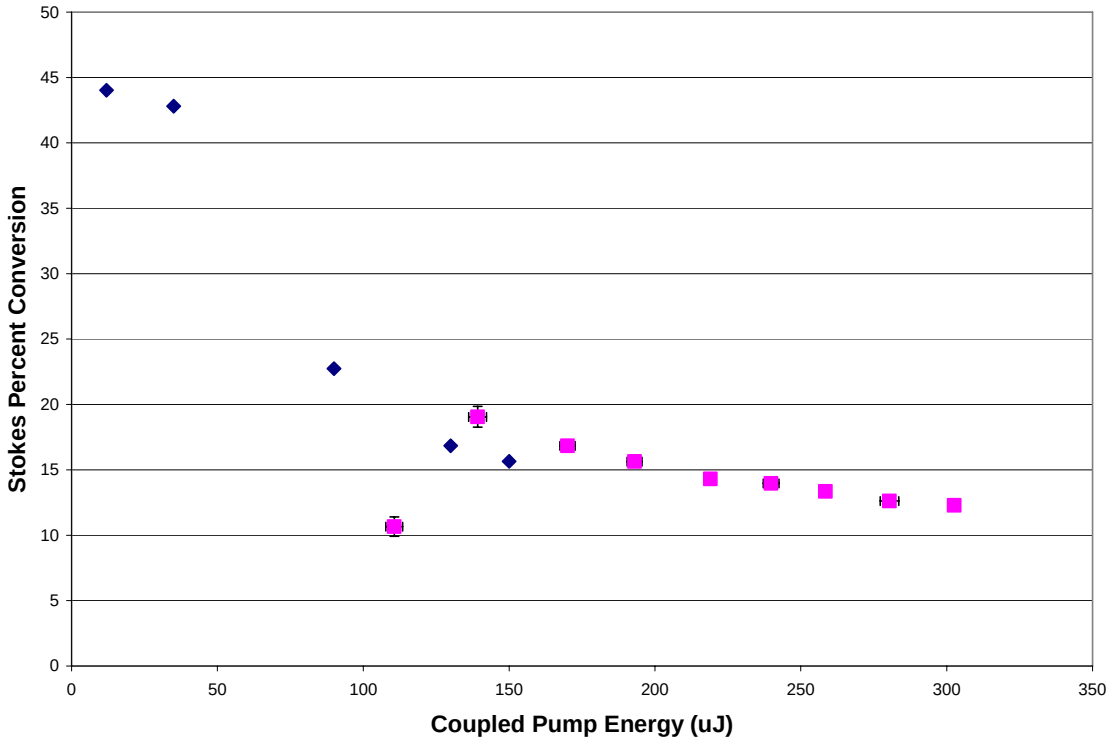

Figure 29. Stokes percent conversion as a function of increasing coupled pump energy for 100 µm fiber (diamonds) and 200 µm fiber (squares).

The graph above demonstrated that the 100 µm fiber had a higher Stokes conversion efficiency, due to the lower Stokes threshold. The decreasing conversion efficiency as power increased was explained by the fiber characteristics of increased attenuation at longer wavelengths.

The fibers were also compared in terms of total Stokes output energy. A larger amount of Stokes energy produced means the fiber is more suitable for beam combining applications requiring higher peak powers. The results demonstrated that although the 100 µm fiber had a lower Stokes threshold, the 200 µm fiber produced more overall

Stokes power. In addition, the Stokes M^2 values in both fibers produced by the combined beam as power was increased were quite similar. Therefore, the higher energy from the 200 μm fiber would result in a higher brightness from that fiber, and would thus be more suitable for higher power applications. The results of these measurements are displayed on the graph below:

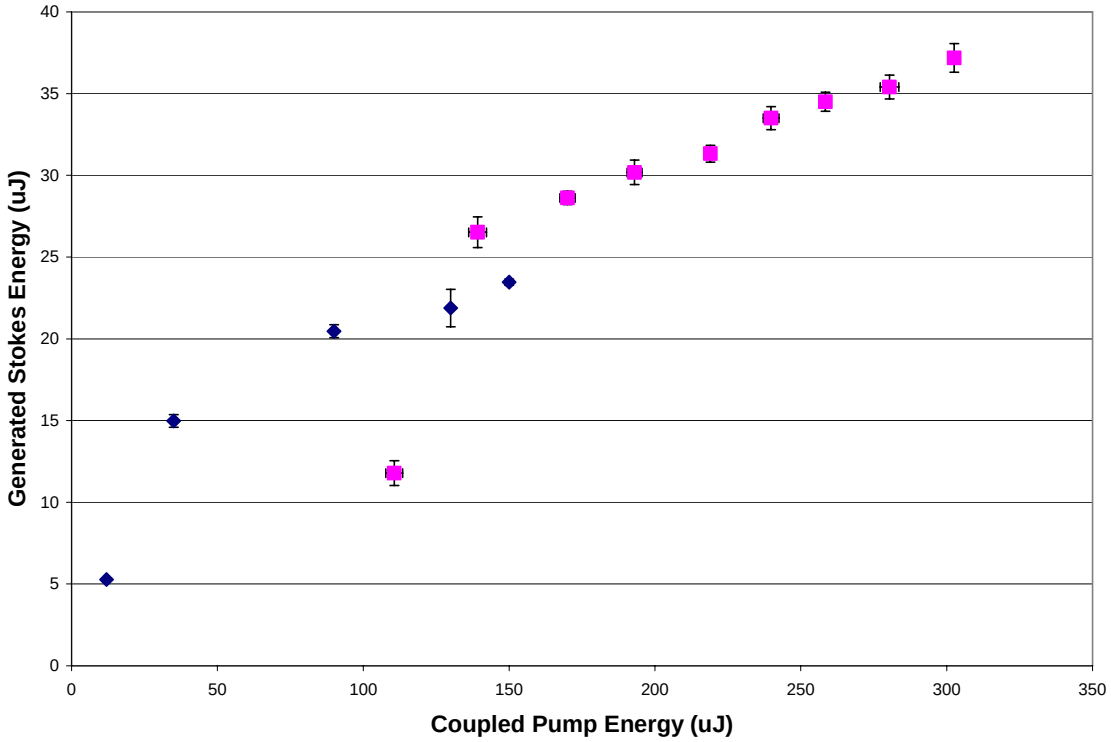

Figure 30. Generated Stokes energy in 100 μm fiber (diamonds) and 200 μm fiber (squares) as a function of pump energy coupled into the fiber.

6.3 Summary

The results of this experiment demonstrated that using a 200 μm fiber, four separate pump beams could be combined into one Stokes beam of good beam quality. The M^2 value produced in the 200 μm fiber (M^2 = 1.40) was an improvement over the optimum value produced in 100 μm fiber (M^2 = 1.86).

In addition, once above the Stokes threshold, M^2 was shown to increase from an optimum value ($M^2 = 1.40$) to a poorer value ($M^2 = 2.82$) with increasing pump energy. The lower quality Stokes beam was explained by higher energy pump beams having more energy in higher order modes, and therefore the value of the overlap integral grew for modes other than the fundamental mode.

Additionally, the pump-to-Stokes conversion efficiency decreased from a high of 19% to a low of 12% as input pump energy increased. This was determined to be due to the higher attenuation characteristics of the SRS fiber at longer wavelengths. Above a certain wavelength, excess pump energy was absorbed by the fiber and lost as heat rather than contributed to higher Stokes orders. The increased absorption meant that little additional Stokes energy was observed as the pump energy was increased, thus the overall conversion efficiency was decreased.

Finally, the performance of the 200 μm fiber was compared to that of the 100 μm fiber. The 100 μm fiber had a lower Stokes threshold, explained by its smaller core diameter. The 100 μm fiber had a higher optimum energy conversion efficiency than the 200 μm fiber, but appeared to have a lower conversion efficiency as input power was increased. Perhaps most importantly for high power applications, the 100 μm fiber had a much lower energy output than the 200 μm fiber.

7 Stokes Beam Quality as Fiber Length Changed

7.1 Experimental Setup

After the beam combination experiments demonstrated the impact of fiber attenuation on output energy, it became apparent that a shorter fiber might increase output energy. However, it seemed important to investigate the impact on beam quality of switching to a shorter fiber, so an experiment was designed to measure beam quality as a function of length in 100 μm fiber. The experimental setup is shown below:

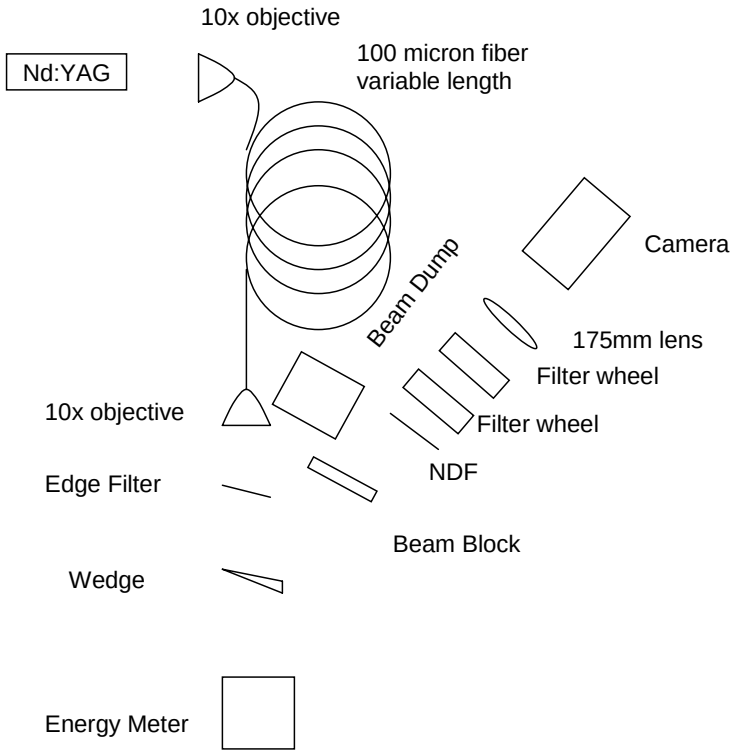

Figure 31. Experimental setup for observing beam cleanup in 100 um core size fiber. The fiber spool was cut to a series of different lengths, and the Stokes beam quality was then measured. The 1064 nm laser light from the Nd:YAG laser served as the pump for the SRS process in the fiber. The edge filter reflected any residual pump light into a beam dump, ensuring no pump light was present when diagnostics where performed. The wedge served as a pickoff, allowing diagnostics but preventing damage to sensitive equipment. The neutral density filter (NDF) attenuated the beam to prevent saturation of the camera. The use of 10x microscope objectives on either end of the fiber resulted in maximum coupling efficiency.

The fiber spool was initially 1.3 km in length, but was shortened in 50 m or 100 m increments to observe the effects of changing length on beam quality. The Nd:YAG laser was set to operate at a pulse repetition rate of 2 kHz. For this experiment, beam quality was measured at both a constant diode pump current on the Nd:YAG laser and at a diode pump current that was two times above the Stokes threshold. The constant diode pump current ensured that the characteristics of the incoming pump laser were uniform throughout the test. However, as the fiber length was shortened, the SRS threshold energy increased. As a result, at a constant pump current, less and less energy was available to transfer to the Stokes beam. Taking additional data points at two times above the Stokes threshold was an attempt to ensure consistency in terms of the Stokes beam characteristics. During this experiment, it became apparent that due to thermal effects, the Nd:YAG laser output power depended on both the diode pump current and the amount of warm-up time the laser was allowed. Because of this, the Stokes threshold was measured immediately before each beam quality measurement so that two times above threshold could be properly calculated.

7.2 Results

As the fiber spool was shortened, two measurements of beam quality were performed at different diode pump current levels. Below 400 m, the effective length of the fiber was too short to achieve the Stokes threshold with pulses produced by 12.9 A of diode pump current.

An anomalous data point must be explained. When the measurement at 300 m was taken, it was the first of that particular day. As a result, the laser had less warm-up

time, so the Stokes threshold was very high in terms of diode pump current. Therefore, when two times above the Stokes threshold was determined, the M^2 measurement was performed at 19.9 A, whereas the typical measurement was performed much closer to 13.5 A. The resulting high M^2 value was consistent with earlier data that shows M^2 deteriorating as pump energy increased. A graph of the beam quality results is shown below:

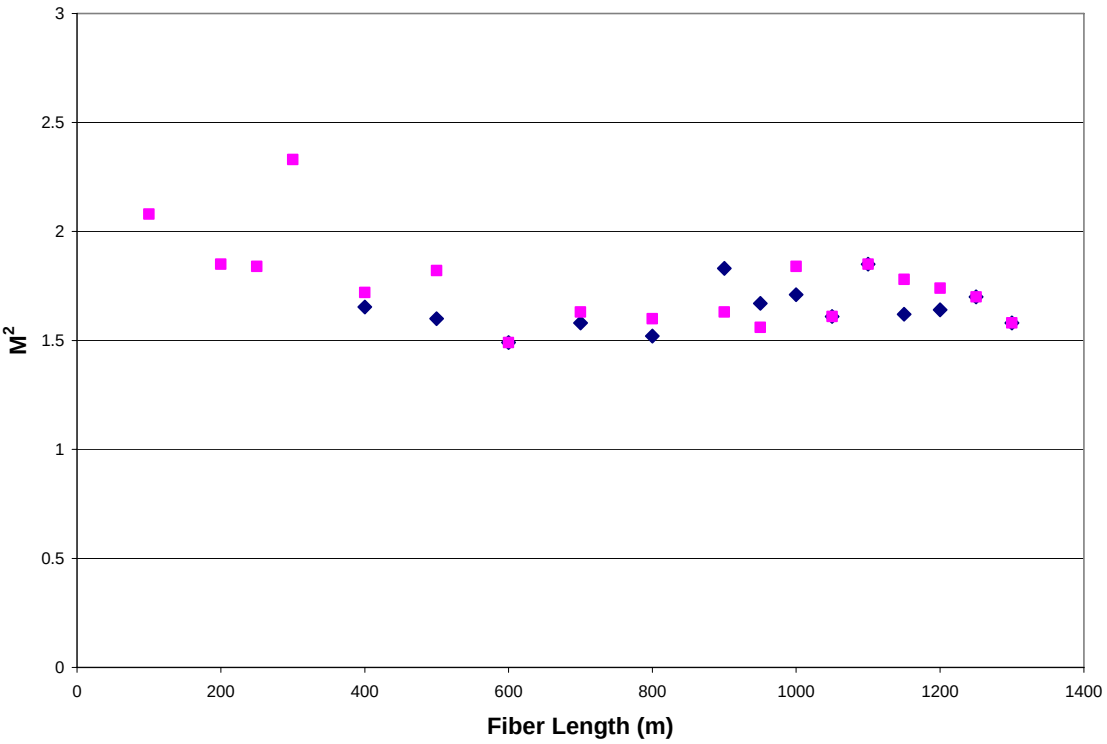

Figure 32. M^2 value of the generated Stokes beam as a function of 100 μm core size fiber length. M^2 values were calculated for a diode pump current on the Nd:YAG pump laser of 12.9 A (diamonds) and two times above the Stokes threshold (squares).

The graph above demonstrated two key points. First, beam quality did slightly degrade when the fiber was less than 400 m in length. This seems consistent with the idea that the fundamental Stokes mode needs some fiber length to exploit its preferential gain and become established. Second, above 400 m, the beam quality remained consistently

between $M^2 = 1.5$ and $M^2 = 2.0$. The implication is that if $M^2 < 2.0$ is acceptable for a particular application, and if the Stokes threshold can be met, there is no benefit to using a longer fiber. The far field pictures taken of the generated Stokes beam for various fiber lengths confirm this and are shown below:

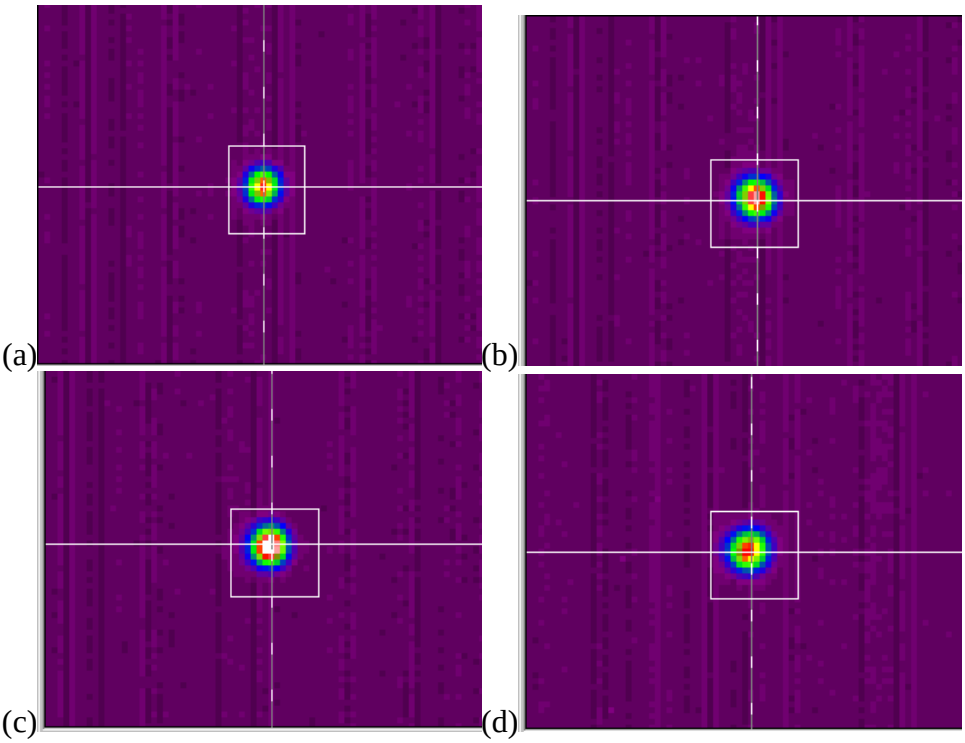

Figure 33. Far field pictures of generated Stokes beam output from 100 μm fiber as a function of length. Pictures were all taken at a pump energy two times above the Stokes threshold. From top left: (a) 1300 m (b) 1000 m (c) 700 m (d) 200 m.

7.3 Summary

This experiment demonstrated the effect of varying the length of a 100 μm fiber spool on beam quality of the generated Stokes beam. Above 400 meters, no improvement in beam quality was observed. For high power applications, the shortest length of fiber close to 400 m should be chosen such that the Stokes threshold can be met and attenuation of the Stokes beam in the fiber is minimized.

8 Graded Index Fiber Compared to Step Index Fiber

8.1 Motivation

In Chiang's 1992 paper, calculations were performed to demonstrate the preferential growth of the fundamental Stokes modes, and various different Stokes modes were demonstrated (3:352). However, the different Stokes modes were demonstrated in graded index fiber, while the calculations were performed for a step index fiber. This difference raised the question of whether the index profile would affect beam cleanup. Since different cladding types produce a different intensity profile in the fiber, a different intensity profile is generated inside the two types of fibers. This resulting intensity profile influences the likelihood of generating SRS in low order modes, and therefore beam cleanup.

8.2 Experimental Setup

In order to compare a step index fiber to the tests previously performed on the 100 μm graded index (GRIN) fiber, a 50 μm step index fiber was selected. The 50 μm fiber had a larger NA (0.365) than the 100 μm fiber (0.29). In order to make a valid comparison, the chosen step index fiber must be similar in both length and number of modes allowed. A calculation of the number of allowed modes begins with the V parameter for a fiber, given by the equation below (10:279):

$$V = 2\pi \frac{a}{\lambda_0} NA \tag{9}$$

In the above equation, a is the radius of the fiber core, λ_0 is the free-space laser wavelength, and NA is the fiber's numerical aperture. However, the number of modes

supported by a given fiber depends on whether the cladding is step index or graded index. For a step index fiber, the number of modes (M) is determined by the expression below (10:293):

$$M \approx \frac{V^2}{2} \tag{10}$$

In contrast to a step index fiber, a GRIN fiber is designed so that all modes travel at the approximately the same velocity. The number of modes (M) for a GRIN fiber is then determined by the expression below (10:296):

$$M \approx \frac{V^2}{4} \tag{11}$$

Using the relationships above, the chosen step index fiber supports about 1452 modes, while the GRIN fiber supports about 1833 modes. This ensures that the energy density in the step index fiber will be higher than in the GRIN fiber.

After calculating the V parameter for both types of fibers, a .365 NA, 50 μm step index fiber spool 900 m in length was identified. A second spool of .29 NA, 100 μm GRIN fiber 900 m in length was also prepared for comparison. Because of the differences in core size and NA, different power objectives were used to achieve optimum coupling efficiency for each fiber.

To ensure operation above the SRS threshold, the Nd:YAG laser was set to a diode pump current of 18.5 A and pulse repetition rate of 1.4 kHz while testing the 100 μm fiber. This resulted in about 27 μJ of Stokes energy per pulse observed at the back end of the fiber. To avoid damaging the 50 μm fiber when the more powerful objectives were used, the laser was set to a diode pump current of 13.5 A and pulse repetition rate of

1.4 kHz. These settings produced about 23 µJ of Stokes energy per pulse out the back end of the fiber. The diagrams below show the experimental setup for the fiber comparison.

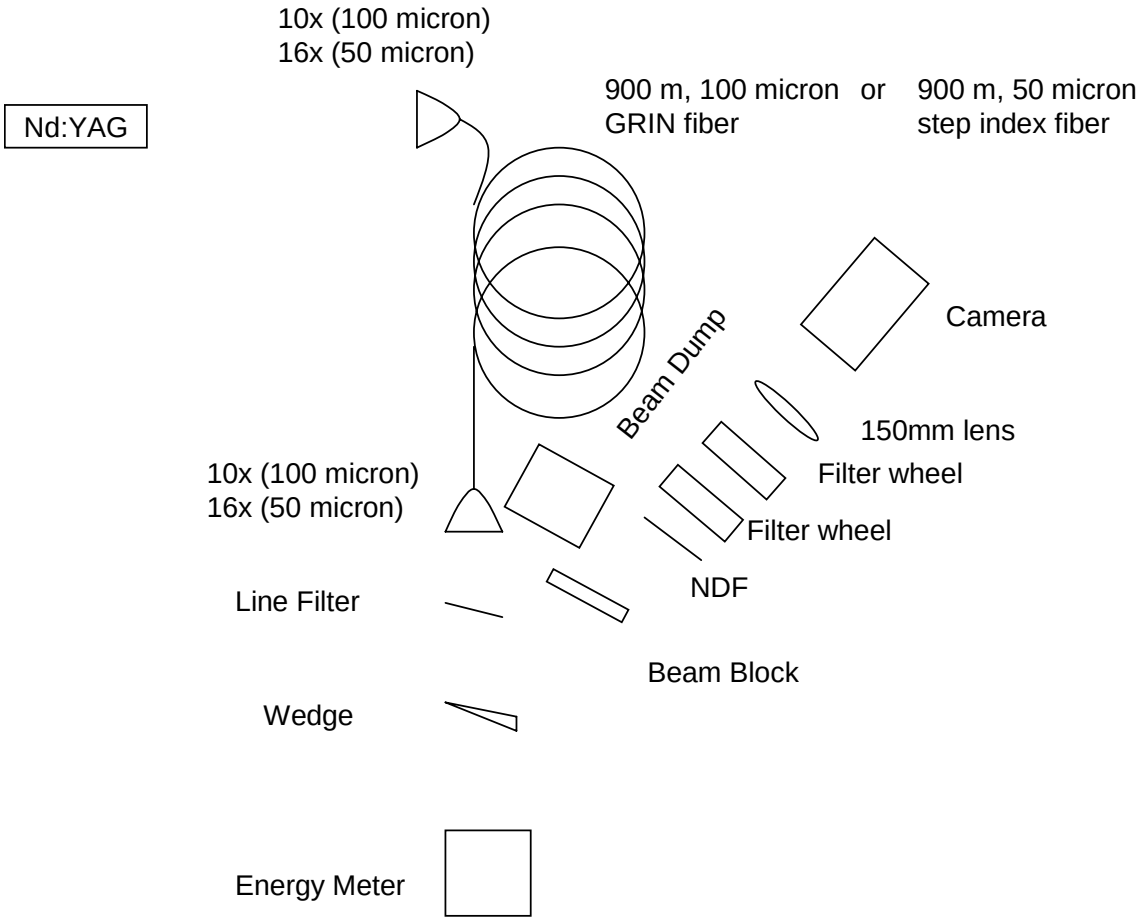

Figure 34. Experimental setup for observing beam cleanup in .29 NA, 100 um graded index (GRIN) and .365 NA, 50 µm step index fiber. The 1064 nm laser light from the Nd:YAG laser served as the pump for the SRS process in the fiber. The edge filter reflected any residual pump light into a beam dump, ensuring no pump light was present when diagnostics where performed. The wedge served as a pickoff, allowing diagnostics but preventing damage to sensitive equipment. The use of 10x microscope objectives on either end of the fiber resulted in maximum coupling efficiency for the 100 µm fiber, but 16x objectives proved ideal for the 50 µm fiber due to the larger NA.

8.3 Results

The beam quality of the generated Stokes and transmitted pump beams were measured for both fibers. In addition, pictures were taken in both the near and far field for each case. The M^2 results are shown below:

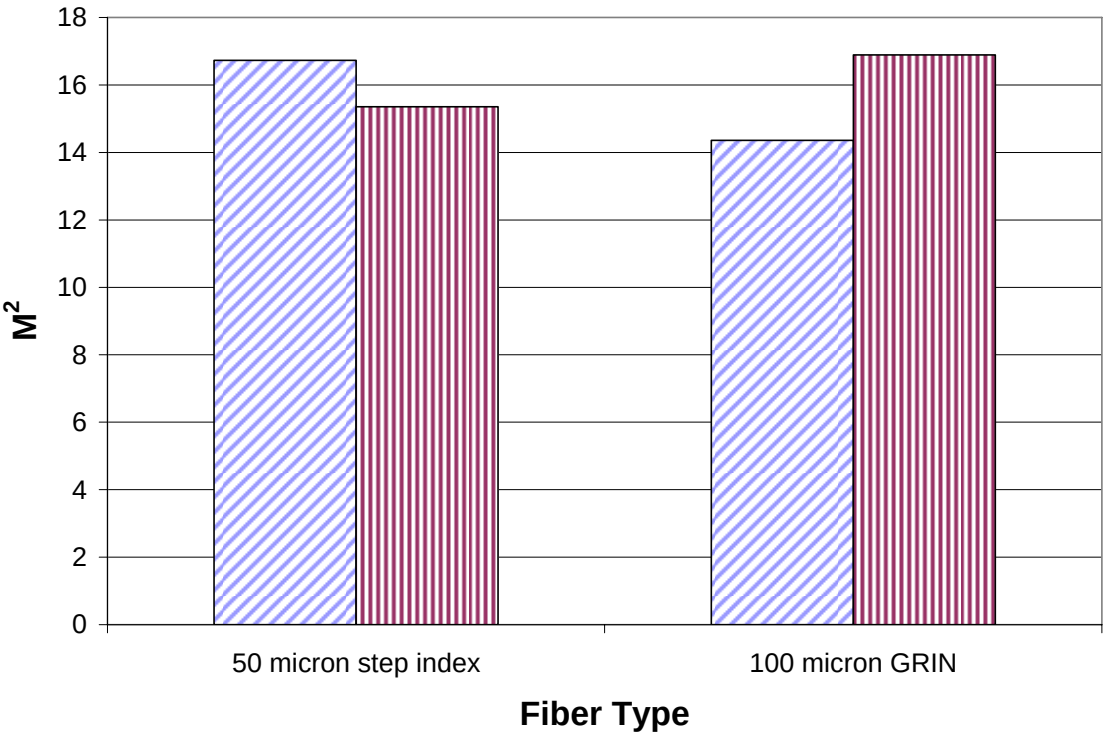

Figure 35. M^2 of generated Stokes beam (diagonal stripes) and transmitted pump beam (vertical stripes) for 50 µm step index fiber and 100 µm graded index (GRIN) fiber.

The M^2 measurements demonstrate that beam cleanup was not achieved in the step index fiber. In fact, the SRS process actually generated a Stokes beam with worse beam quality than the transmitted pump beam (M^2_{pump} = 16.73, M^2_{Stokes} = 14.36). In the case of the GRIN fiber, the beam quality of the generated Stokes beam was slightly better than the transmitted pump beam (M^2_{pump} = 16.89, M^2_{Stokes} = 15.35).

Beam quality was also observed by taking pictures in both the near and far field for each fiber. The results of the step index fiber are shown below:

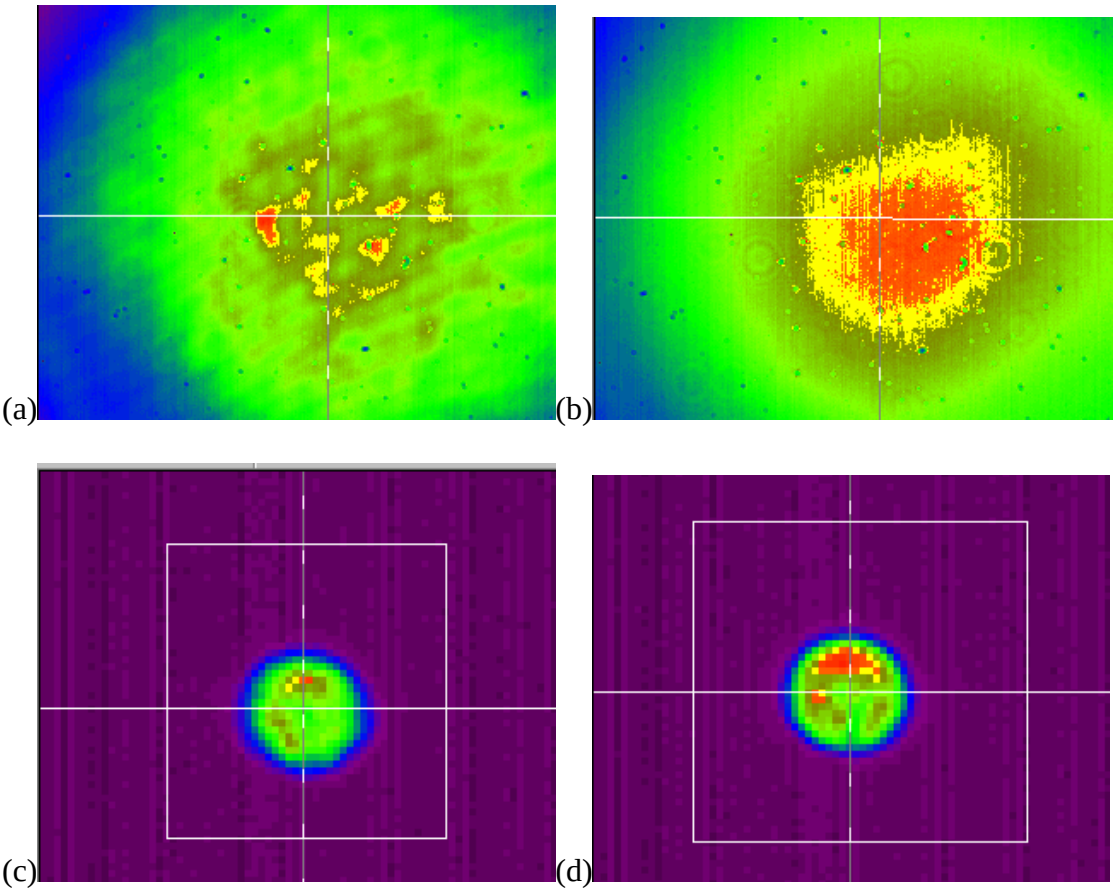

Figure 36. Pictures of the output from the 50 µm step index fiber, allowing comparison of generated Stokes beam to transmitted pump beam. The far field pictures are with 4x zoom, while no zoom is applied for the near field. (a) Near field transmitted pump beam (b) Near field generated Stokes beam (c) Far field transmitted pump beam (d) Far field generated Stokes beam

The pictures above confirm the M^2 measurements showing no beam cleanup occurred. For example, similar intensity profiles and beam sizes were observed in the far field for both the transmitted pump and generated Stokes beam.

For the GRIN fiber, pictures of the beams confirm the M2 measurements and suggest that a small amount of beam cleanup occurred, as a more uniform intensity

profile and smaller spot size in the far field were produced. The pictures below display the generated Stokes beam and transmitted pump beam for the GRIN fiber:

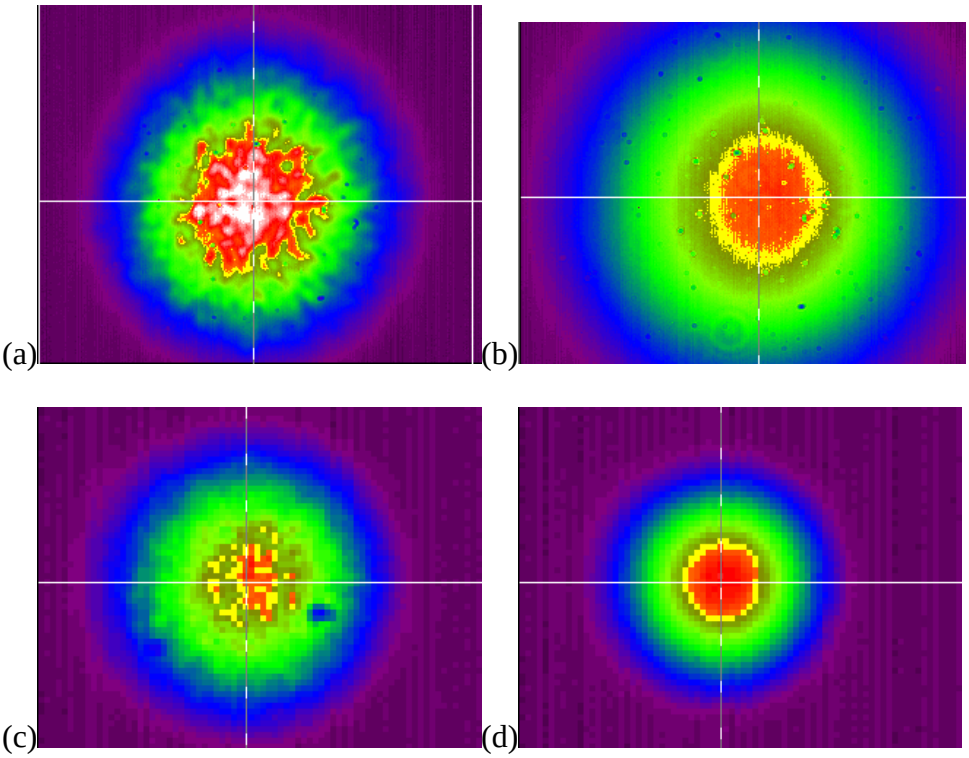

Figure 37. Pictures of the output from the 100 µm graded index fiber, allowing comparison of generated Stokes beam to transmitted pump beam. The far field pictures are with 4x zoom, while no zoom is applied for the near field. (a) Near field transmitted pump beam (b) Near field generated Stokes beam (c) Far field transmitted pump beam (d) Far field generated Stokes beam

8.4 Summary

In the step index fiber, the SRS process actually generated a Stokes beam with worse beam quality than the transmitted pump beam (M^2_{pump} = 16.73, M^2_{Stokes} = 14.36). In the case of the GRIN fiber, the beam quality of the generated Stokes beam was slightly better than the transmitted pump beam (M^2_{pump} = 16.89, M^2_{Stokes} = 15.35).

However, the small amount of beam cleanup observed in the GRIN fiber is in conflict with the results produced during the experiments described in Chapter 7, where M^2 of the generated Stokes beam in a different GRIN fiber with the same specifications

was measured as a function of length. In that experiment, at 900 m, generated Stokes beam M^2 values of 1.83 and 1.63 were produced at two different pump power levels. The differences between these two experiments suggest that the particular fiber used for this experiment was marred by some sort of defect.

In addition to only testing one particular length and fiber combination, given the fact that a defect is suspected to have disrupted the beam cleanup process in the GRIN fiber, a conclusion cannot be drawn about the impact of cladding type on beam cleanup. What can be said is that beam cleanup was not observed in this particular 50 μm step index fiber.

9 Conclusions and Recommendations

9.1 Conclusions of Research

A number of conclusions may be drawn from the experiments performed during the course of this research. Beam combination was demonstrated by splitting the beam from a Q-switched Nd:YAG laser and pumping a multiple input, single output fiber squid. Beam cleanup of the resulting output beam using SRS was then demonstrated in both 100 μm fiber (M^2 = 1.86) and 200 μm fiber (M^2 = 1.40). Energy conversion efficiency into the Stokes beam was measured as a function of input energy and found to be limited by the attenuation characteristics of the fiber. Beam quality was measured via the M^2 fit parameter as a function of input energy and was found to slightly degrade in both fibers as input energy increased. In addition, beam quality was measured as a function of 100 μm fiber length and determined to degrade slightly at fiber lengths less than 400 m. Additional fiber length beyond 400 m did not improve beam quality and reduced output energy, although the Stokes threshold was reduced.

9.1.1 Beam Combination Conclusions

The fiber squid was determined to be an effective tool for overlapping four separate pump beams spatially, and the resulting beam was cleaned up through SRS in both 100 μm fiber (M^2 = 1.86) and 200 μm fiber (M^2 = 1.40). Experimentation determined that the beam produced by different input channels of the fiber squid produced varying degrees of beam cleanup and Stokes conversion efficiency, which was likely due to slight differences in the overlap of the pump beam leaving the fiber squid with the fundamental Stokes mode of the SRS fiber. These overlap differences were

demonstrated because for any two input channels, the generated Stokes beam quality could sometimes be predicted by a weighted average of both the M^2 values of each channel individually, but in other cases the weighted average was not a good predictor of beam quality. The overlap differences are likely due to the physical construction of the fiber squid, where different input channels are fused at different points on the squid.

9.1.2 Stokes Conversion Efficiency Conclusions

When input energy was increased, the conversion efficiency of pump energy to Stokes energy decreased. In the 100 μm fiber, the pump-to-Stokes conversion efficiency decreased from a high of 44% to a low of 16% as input pump energy increased. In the 200 μm fiber, the pump-to-Stokes conversion efficiency decreased from a high of 19% to a low of 12% as input pump energy increased. For a given input pump energy in the range where the two fibers overlap, the 200 μm fiber was more efficient than the 100 μm fiber.

9.1.3 Beam Quality Conclusions

Once above the Stokes threshold, M^2 was shown to increase in 100 μm fiber from an optimum value ($M^2 = 1.86$) to the worst value ($M^2 = 2.64$) with increasing pump energy. This decrease in beam quality was also observed in the 200 μm fiber. The optimum value ($M^2 = 1.40$) was seen just above the Stokes threshold, with beam quality decreasing ($M^2 = 2.82$) as pump energy increased. The lower quality Stokes beam was explained by higher energy pump beams having more energy in higher order modes, and therefore the value of the overlap integral grows for modes other than the fundamental mode.

The performance of the 200 μm fiber was compared to that of the 100 μm fiber. The 100 μm fiber had a lower Stokes threshold, explained by its smaller core diameter. The 100 μm fiber had a higher optimum energy conversion efficiency than the 200 μm fiber, but appeared to have a lower conversion efficiency as input power was increased. Perhaps most importantly for high power applications, the 100 μm fiber had a much lower energy output than the 200 μm fiber.

Finally, an experiment demonstrated the effect of varying the length of a 100 μm fiber spool on beam quality of the generated Stokes beam. Above 400 m, no improvement in beam quality was observed. When the fiber spool was shortened below 400 m, beam quality began to slightly degrade ($M^2 < 2.5$).

9.2 Recommendations for Future Research

A major shortcoming of this research was the inability to combine multiple high energy input beams efficiently. The decrease in efficiency seen at higher energies was attributed to the varying attenuation characteristics of the SRS fiber, which increased dramatically for longer wavelengths. As the energy per pulse increased, more energy was shifted into the higher Stokes orders, and therefore attenuated along the length of the fiber. The increased absorption meant that very little additional Stokes energy was observed as the pump energy was increased, thus the overall conversion efficiency was decreased.

Future work should focus on eliminating four-wave mixing to increase the thresholds of higher Stokes orders, and thereby reduce the amount of energy coupled into those higher orders which are in turn so quickly absorbed by the fiber. This could perhaps

be achieved by using a backwards SRS geometry, where a small Stokes seed of good beam quality could be coupled into the back end of a length of fiber for amplification. Multiple high power sources could be combined using the fiber squid, and the output of the fiber squid could then be coupled into the front end as a pump of the fiber with the seeded back end. This backwards geometry prevents four-wave mixing because the phase matching conditions cannot be met.

A second area for future work would be to address the uneven attenuation characteristics of the fiber. If a constant attenuation profile can be produced over a wide wavelength region, then the current geometry may prove suitable.

Finally, for high power applications, the shortest length of fiber close to 400 m should be chosen such that the Stokes threshold can be met and attenuation of the Stokes beam in the fiber is minimized. If fiber shorter than the ~2 km spools used in this research were employed, attenuation of the Stokes beam would be reduced dramatically, and perhaps the resulting efficiency would prove suitable.

Bibliography

1. Agrawal, Govind P. *Nonlinear Fiber Optics*. New York: Academic Press, 2001.

2. Azar, Maurice C. *Assessing The Treatment Of Airborne High Energy Lasers in Combat Simulations*. MS thesis, AFIT/GOR/ENS/03-02, Graduate School of Management and Engineering, Air Force Institute of Technology (AU), Wright-Patterson AFB OH, March 2003.

3. Chiang, K. S., *Optics Letters*, Vol. 17, 352 (1992).

4. Eichler, H. J., A. Haase and O. Mehl, in *High Power Lasers – Science and Engineering*, eds. R. Kossowsky, M. Jelinek, and R. F. Walter. Boston: Kluwer Academic Publishers, 1996.

5. Horiba Jovin Yvon website, http://www.jobinyvon.com/usadivisions/OOS/oos3.htm, Dec 2005

6. Marcuse, D., "Loss analysis of single mode fiber splices", *The Bell Sys. Tech. J.* 56, No. 6, 703-718, (1977).

7. Murray, J. T., W. L. Austin, and R. C. Powell, *Optical Materials*, Vol. 11, 353-371 (1999)

8. OFS Fiber specification sheet for 100 μm core, graded index multimode fiber.

9. Russell, T. H., S. M. Willis, M. B. Crookston, and W. B. Roh, *Journal of Nonlinear Optical Physics & Materials*, Vol. 11, No. 3, 303-316, (2002).

10. Saleh, Bahaa E. A., and Malvin C. Tech, *Fundamentals of Photonics*. New York: Wiley-Interscience, 1991.

11. Yariv, Amnon and Pochi Yeh, *Optical Waves in Crystals*. Hoboken: Wiley-Interscience, 2003.

REPORT DOCUMENTATION PAGE

Form Approved
OMB No. 074-0188

1. REPORT DATE *(DD-MM-YYYY)*	2. REPORT TYPE	3. DATES COVERED *(From – To)*
17-02-2006	Master's Thesis	August 2005 – March 2006

4. TITLE AND SUBTITLE

DEVELOPMENT OF A MULTIPLE BEAM COMBINER USING STIMULATED RAMAN SCATTERING IN MULTIMODE FIBER

5a. CONTRACT NUMBER

5b. GRANT NUMBER

5c. PROGRAM ELEMENT NUMBER

6. AUTHOR(S)

Flusche, Brian M., 1st Lt, USAF

5d. PROJECT NUMBER
NAFRL056209093

5e. TASK NUMBER

5f. WORK UNIT NUMBER

7. PERFORMING ORGANIZATION NAMES(S) AND ADDRESS(S)
Air Force Institute of Technology
Graduate School of Engineering and Management (AFIT/EN)
2950 Hobson Way, Building 640
WPAFB OH 45433-8865

8. PERFORMING ORGANIZATION REPORT NUMBER

AFIT/GAP/ENP/06-04

9. SPONSORING/MONITORING AGENCY NAME(S) AND ADDRESS(ES)
AFRL/DELO
ATTN: Rick Berdine
3550 Aberdeen Ave SE, Kirtland, AFB 87117-5776
505-853-4342

10. SPONSOR/MONITOR'S ACRONYM(S)

11. SPONSOR/MONITOR'S REPORT NUMBER(S)

12. DISTRIBUTION/AVAILABILITY STATEMENT

APPROVED FOR PUBLIC RELEASE; DISTRIBUTION UNLIMITED.

13. SUPPLEMENTARY NOTES

14. ABSTRACT

Beam combination was demonstrated by splitting the beam from a Q-switched Nd:YAG laser and pumping a multiple input, single output fiber squid. Beam cleanup of the resulting output beam using stimulated Raman scattering was then demonstrated in both 100 μm fiber and 200 μm fiber. Energy conversion efficiency into the Stokes beam was measured as a function of input energy and found to be limited by the attenuation characteristics of the fiber. Beam quality was measured via the M^2 fit parameter as a function of input energy and was found to slightly degrade in both fibers as input energy increased. In addition, beam quality was measured as a function of 100 μm fiber length and determined to degrade slightly at fiber lengths less than 400 m. Additional fiber length beyond 400 m did not improve beam quality and reduced output energy, although the Stokes threshold was reduced. The performance of the 200 μm fiber was compared to that of the 100 μm fiber.

15. SUBJECT TERMS
Stimulated Raman Scattering, Fiber Optics, Nonlinear Optics, Beam Quality

16. SECURITY CLASSIFICATION OF:			17. LIMITATION OF ABSTRACT	18. NUMBER OF PAGES	19a. NAME OF RESPONSIBLE PERSON
a. REPORT	b. ABSTRACT	c. THIS PAGE			Thomas Alley, Lt Col, USAF
U	U	U	UU	80	19b. TELEPHONE NUMBER *(Include area code)* (937) 255-3636, ext 4649 (thomas.alley@afit.edu)